

Gleeok's Fire-breathing: Triple Flares of AT 2021aek within Five Years from the Active Galaxy SDSS J161259.83+421940.3

DONG-WEI BAO[†],¹ WEI-JIAN GUO[†],^{1,2} ZHI-XIANG ZHANG[†],³ CHENG CHENG[†],⁴ ZHU-HENG YAO[†],^{5,6} YAN-RONG LI[†],⁷
YE-FEI YUAN[†],⁸ SUI-JIAN XUE,^{1,2} JIAN-MIN WANG[†],⁷ CHAO-WEI TSAI[†],^{9,10,11} HU ZOU[†],^{1,2} YONG-JIE CHEN[†],⁷
WENXIONG LI[†],^{1,2} SHIYAN ZHONG[†],¹² AND ZHI-QIANG CHEN[†]¹³

¹National Astronomical Observatories, Chinese Academy of Sciences, 20A Datun Road, Chaoyang District, Beijing 100101, China, sgkmdks@gmail.com

²Key Laboratory of Optical Astronomy, National Astronomical Observatories, Chinese Academy of Sciences, Beijing 100012, China

³Department of Astronomy, Xiamen University, Xiamen, Fujian 361005, People's Republic of China, zhangzx@xmu.edu.cn

⁴Chinese Academy of Sciences South America Center for Astronomy, National Astronomical Observatories, CAS, Beijing 100101, China, chengcheng@nao.cas.cn

⁵Key Laboratory for Particle Astrophysics, Institute of High Energy Physics, Chinese Academy of Sciences, 19B Yuquan Road, Beijing 100049, China

⁶School of Physical Science, University of Chinese Academy of Sciences, 19A Yuquan Road, Beijing 100049, People's Republic of China

⁷Key Laboratory for Particle Astrophysics, Institute of High Energy Physics, Chinese Academy of Sciences, 19B Yuquan Road, Beijing 100049, People's Republic of China

⁸Department of Astronomy, University of Science and Technology of China, Hefei 230026, Anhui, China

⁹National Astronomical Observatories, Chinese Academy of Sciences, 20A Datun Road, Beijing 100101, China

¹⁰Institute for Frontiers in Astronomy and Astrophysics, Beijing Normal University, Beijing 102206, China

¹¹School of Astronomy and Space Science, University of Chinese Academy of Sciences, Beijing 100049, China

¹²South-Western Institute for Astronomy Research, Yunnan University, Kunming, 650500 Yunnan, People's Republic of China

¹³School of Physics and Technology, Nanjing Normal University, No. 1, Wenyuan Road, Nanjing, 210023, People's Republic of China

ABSTRACT

We present a noteworthy transient AT 2021aek exhibiting three distinct optical flares between 2018 and 2023. It is hosted in a radio-loud narrow-line Seyfert 1 (NLSy1) galaxy, with an optical image showing a minor tidal morphology and a red mid-infrared color ($W1 - W2 = 1.1$). Flares II and III exhibit rapid rises, and long-term decays ($\gtrsim 1000$ days) with recurring after-peak bumps. The $g-r$ color after subtracting the reference magnitude exhibited a rapid drop and recovery during Flare II, followed by the minor after-peak evolution in blue colors. We applied a canonical tidal disruption event (TDE) fitting on the light curves which gives a decay index p of $-2.99^{+0.13}_{-0.14}$ for Flare II and $-1.61^{+0.34}_{-0.65}$ for Flare III. The blackbody fitting shows lower temperatures ($\sim 10^{3.8}$ K) with minor after-peak evolution. The blackbody radius ($\gtrsim 10^{16}$ cm) and luminosity ($\sim 10^{45}$ erg s⁻¹) are larger than the typical TDE sample's. The time lag (in rest frame) between ZTF g - and r -band ($\tau_{g,r} = 3.4^{+1.0}_{-0.9}$ days) significantly exceeds the prediction from the standard accretion disk. Pre-burst spectra reveal prominent Bowen fluorescence lines, indicating a vigorous or potentially long-lasting process that enriches the local metallicity. Additionally, we derived black hole masses of $\log M_{\bullet} = 7.09^{+0.18}_{-0.31} M_{\odot}$ and $\log M_{\bullet} = 7.52^{+0.08}_{-0.10} M_{\odot}$ using $H\beta$ and $H\alpha$ emission lines. The variation and recurring features of AT 2021aek are not likely induced by the radio-beaming effect or Type-II superluminous supernova (SLSN-II), however, we cannot rule out the possibility of TDE or enhanced active galactic nuclei (AGN) accretion process. The unusually high occurrence of three flares within five years may also be induced by the complex local environment.

Keywords: Accretion (14); Active galactic nuclei (16); Supermassive black holes (1663); Tidal disruption (1696);

1. INTRODUCTION

The emergence of automated photometry surveys, such as the Catalina Survey (CRTS; Drake et al. 2009), All-Sky Automated Survey for SuperNovae (ASAS-SN; Kochanek et al. 2017), the Zwicky Transient Facility (ZTF; Masci et al. 2019), the Asteroid Terrestrial-impact Last Alert System (ATLAS; Tonry et al. 2018), and Pan-STARRS1 (PS1; Chambers et al. 2016), has significantly expanded the

number of optical transients in recent years. This allows for the further study of a wide range of transient phenomena, such as blazars, supernovae (SNe), TDEs, intrinsic variability in AGN, and microlensing events. The physical mechanisms underlying optical transients can be complex and coupled together, which lead to intricate behaviors in the multi-wavelength light curves and spectra, deviating from the typical patterns for individual phenomena. By carefully analyzing these transients and comparing them to known

classes of objects, we can gain valuable insights into the physical properties of their progenitors and the surrounding environments that give rise to them. Below, we present an overview of some optical variability patterns and proposed theoretical models that can induce optical flares.

Blazars are distinguished with their relativistic jets pointed close to our line of sight (Wolfe 1978). This alignment leads to the Doppler beaming, which significantly amplifies the emission across observed wavelengths. The optical emission coming from the synchrotron emission from relativistic electrons in the jet (Konigl 1981; Urry & Mushotzky 1982) is polarized and usually displays remarkable variability on timescales ranging from minutes to decades (e.g., Raiteri et al. 2003; Rani et al. 2010; Gopal-Krishna et al. 2011; Goyal et al. 2018; Chand & Gopal-Krishna 2022). Several models have been proposed to explain the observed variability, including shocks within the jet (Marscher & Gear 1985; Hughes et al. 1985), turbulence and magnetic reconnection (e.g., Guo et al. 2016; Kagan et al. 2015), interaction with external sources (e.g., Araudo et al. 2010; Zacharias et al. 2017), and changes in viewing geometry (e.g., Larionov et al. 2013). More comprehensive reviews can be found in Böttcher (2019); Hovatta & Lindfors (2019).

TDEs (Rees 1988; Evans & Kochanek 1989; Phinney 1989) happen when a star wanders into the tidal radius of a black hole and is torn apart by the gravitational force. Recent advancements in optical sky patrol surveys have led to a significant increase in the number of TDEs detected in the optical band (van Velzen et al. 2020, 2011; Gezari 2012; van Velzen et al. 2021; Hammerstein et al. 2023; Yao et al. 2023). These events exhibit a characteristic rapid rise to peak brightness followed by a gradual decline. The observed slow decline is thought to reflect the gradual fallback of debris streams. As these streams fall back towards the black hole, they self-intersect (relativistic precession effects are involved) and dissipate energy. This process theoretically expects a power-law decline with a slope of $\sim t^{-5/3}$ (Rees 1988; Phinney 1989; Evans & Kochanek 1989). Notably, observation of many TDEs has generally confirmed this theoretical prediction. However, the measured temperature is consistently lower than expected in the predictions of the standard disk theory, and the post-peak minor evolution also deviates from what is expected. This energy discrepancy poses a significant challenge to the understanding of the physical mechanisms responsible for the optical emission in TDEs. To address this controversy, researchers have proposed several alternative models, including envelopes of reprocessing layers (Loeb & Ulmer 1997; Guillochon et al. 2014; Roth et al. 2016; Metzger & Stone 2016; Metzger 2022), shock collision arising from stream self-interaction (Shiokawa et al. 2015; Piran et al. 2015; Guo et al. 2023a), outflow involved to remove mass from the accretion disk (Miller 2015), etc. These models offer potential explanations for the observed discrepancy.

The TDE identification from automated optical surveys typically excludes transients originating from galaxies known to host an AGN to minimize confusion with

AGN variability, which might lead to overlooking TDEs within AGN environments. Recent models offer different perspectives on the impact of AGN accretion disks on TDE rates. Some research (Karas & Šubr 2007; McKernan et al. 2022; Prasad et al. 2024; Wang et al. 2024; Kaur & Stone 2024) suggests that the presence of an AGN accretion disk can potentially lead to an enhanced TDE rate with secular evolution of stellar orbits.

Recent studies have identified an increasing number of optical transients that exhibit characteristics similar to TDEs but in a rather long-term flaring state, which is likely associated with an AGN hosted in the galaxy (Kankare et al. 2017; Blanchard et al. 2017; Trakhtenbrot et al. 2019; Jiang et al. 2019; Gromadzki et al. 2019; Neustadt et al. 2020; Frederick et al. 2021; Cannizzaro et al. 2022; Makrygianni et al. 2023; Petrushevska et al. 2023; Wiseman et al. 2024; Hinkle et al. 2024). These transients often exhibit a rapid rise followed by a prolonged decay lasting over hundreds or thousands of days, deviating from the typical light curve patterns expected for canonical TDEs (van Velzen et al. 2021; Hammerstein et al. 2023). The physical origins of these transients remain uncertain due to the similarities in their multi-wavelength properties with other energetic phenomena such as TDE, SLSN-II, and intrinsic AGN flares. CSS 100217, a transient event located within an NLSy1 galaxy with significant star formation activity, initially drew attention due to its unusually bright optical flare, reaching a peak magnitude of $M_{v(\text{peak})} = -22.7$ mag surpassing the brightness of most known TDEs. Initially classified as an extremely luminous type-II supernova (SN-II) based on its early observations (Drake et al. 2009), CSS 100217 has recently been reclassified as a potential TDE candidate (Cannizzaro et al. 2022). This re-classification is primarily motivated by the fact that the after-decay brightness of CSS 100217 is fainter than its pre-burst brightness. This suggests that the central black hole in the host galaxy is in a relatively low accretion state. A possible explanation for this fainter after-decay brightness is the formation of a cavity in the accretion disk during the TDE event of stars on retrograde orbits (McKernan et al. 2022). Similar fainter brightness can be found in AT 2019brs (Frederick et al. 2019), AT 2021loi (Makrygianni et al. 2023) and AT 2019aalc (Veres et al. 2024) (Quick comparison can be found in Fig.7). PS 16dtm, residing in an NLSy1 galaxy of $M_{\text{BH}} \sim 10^6 M_{\odot}$, exhibited a double-peak plateau during the peak luminosity followed by a smooth decline lasting over 7 years. Initially classified as an SLSN-II (Terreran et al. 2016; Dong et al. 2016), PS 16dtm was later reconsidered as a potential TDE candidate (Blanchard et al. 2017; Petrushevska et al. 2023). Several other long-term-decay transients, including AT 2019brs in Frederick et al. (2019) and ZTF19aamrjar in Wiseman et al. (2024), have also been identified at pre-burst within galaxies known to host AGNs, which give rise to the question of whether an AGN is involved in these long-evolving behaviors. For some long-evolving transients in AGNs, Trakhtenbrot et al. (2019) provided an alternative interpretation that the flares are induced by intrinsic AGN

variability, potentially triggered by a sudden enhancement or re-ignition of a supermassive black hole (SMBH). A key characteristic of these ambiguous transients (Trakhtenbrot et al. 2019; Tadhunter et al. 2017; Blanchard et al. 2017; Frederick et al. 2021; Makrygianni et al. 2023; Veres et al. 2024) is the emergence of Bowen fluorescence (BF) lines during the flaring phase (Bowen 1928; Netzer et al. 1985) which is induced by the presence of intense UV radiation. Dgany et al. (2023) suggest that the BF flares are rare among SMBH-related transients.

Unfortunately, pre-burst observations are often unavailable for many optical transients, making it difficult to definitively confirm the presence of an AGN. PS1-10adi, for example, exhibits a slow, long-term (~ 4 year) decay with a follow-up rebrightening phase (Kankare et al. 2017; Jiang et al. 2019). The emergence of broad Balmer emission lines, Fe II continuum, and Mg II features in the spectrum of PS1-10adi can be attributed to TDE, AGN activity, or an SN-II event. Some ambiguous/extremely nuclear transients (ANTs/ENTs) have been identified in galaxies with tremendous energy released but without any clear sign of AGN activity (Somalwar et al. 2023; Hinkle et al. 2024; Wiseman et al. 2024). It is worth noting that some long-evolving transients even show recurring flares (Jiang et al. 2019; Payne et al. 2021; Soraisam et al. 2022; Somalwar et al. 2023; Makrygianni et al. 2023; Veres et al. 2024). The underlying physical processes driving these new transients remain poorly understood, largely due to the limited number of known examples. However, the discovery of additional long-evolving transients will be crucial for understanding the physical properties of progenitors and the transient demography.

In this paper, we report a serendipitous discovery of an ambiguous transient named AT 2021aeuk in SDSS J161259.83+421940.3, in which three flares occurred within 5 years, and the second flare displayed a long decline $\gtrsim 1000$ days. We compile the archived light curves and spectra aiming at placing constraints on the possible physical origins of these flares. Section 2 presents the archived photometry data and calibration. Section 3 presents the measurement and analysis for light curves and spectra. In Section 4, we discuss the possible physical mechanism for AT 2021aeuk. In Section 5, we present the summary. Throughout, we adopt a Λ CDM cosmology with $H_0 = 67 \text{ km s}^{-1} \text{ Mpc}^{-1}$, $\Omega_\Lambda = 0.68$, and $\Omega_m = 0.32$ (Planck Collaboration et al. 2020).

2. DATA COLLECTION AND PROCESSING

2.1. Basic Information

The host galaxy of AT 2021aeuk, SDSS J161259.83+421940.3 (hereafter J1612), is classified as a radio-loud ($\log R^* \sim 1.06$ from Whalen et al. 2006) NLSy1 galaxy (White et al. 2000) at a redshift of 0.234. It is optically blue while bright in the infrared wavelengths with differential magnitudes $W1 - W2 = 1.1$, $W3 - W4 = 2.569$ archived from the *Wide-field Infrared Survey Explorer* (WISE) which suggests an origin of the reprocessing from hot

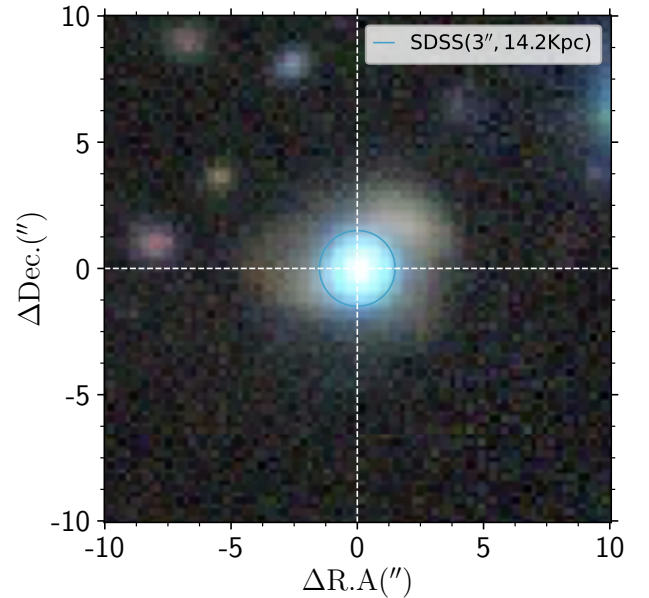


Figure 1. The $g-r-i$ false-color image of AT 2021aeuk captured by the Subaru/HSC (Aihara et al. 2022). The depth of the r band image is about 26 AB mag. The SDSS fiber aperture with diameter of $3''$ is denoted by the blue circle, corresponding to a scale of 14.2 kpc.

dust by AGN (Stern et al. 2005). The irregular morphology revealed in the Subaru/Hyper Suprime-Cam (HSC) color image (Fig.1) indicate that J1612 might have experienced a galaxy merger event. The high-resolution Very Large Array (VLA) observations at 5 GHz (beam size of $1'' \times 0.42''$) show two ambiguous radio cores with a separation of about 2 kpc (Berton et al. 2018), which are not resolved by the HSC with a resolution of $0.7''$.

2.2. Light Curve and Calibration

Various archived photometry data from different telescopes were collected to extend the light curve, including ZTF, ASAS-SN, ATLAS, CRTS, and PS1. The photometry data are presented in Fig. 2.

Due to different apertures and filters, the photometry data from archived surveys require inter-calibration to present the long-term variation. The inter-band flux scaling is conducted using the Bayesian package PyCALI¹ (Li et al. 2014), which fits the light curves with a damped random walk process (Kelly et al. 2009; MacLeod et al. 2010; Zu et al. 2013) and employs Markov Chain Monte Carlo (MCMC) to recover the normalization parameters and uncertainties for data from different telescopes. We scaled all photometry data to ZTF r -band. However, we note that there is no sampling overlap around MJD 57000 between the datasets from CRTS/PS1 and ASAS-SN/ATLAS/ZTF. Therefore, the flux scaling is not performed for datasets from CRTS/PS1 (see grey points in Panel b in Fig.2). Nevertheless, this does not affect our

¹ <https://github.com/LiyrAstroph/PyCALI>

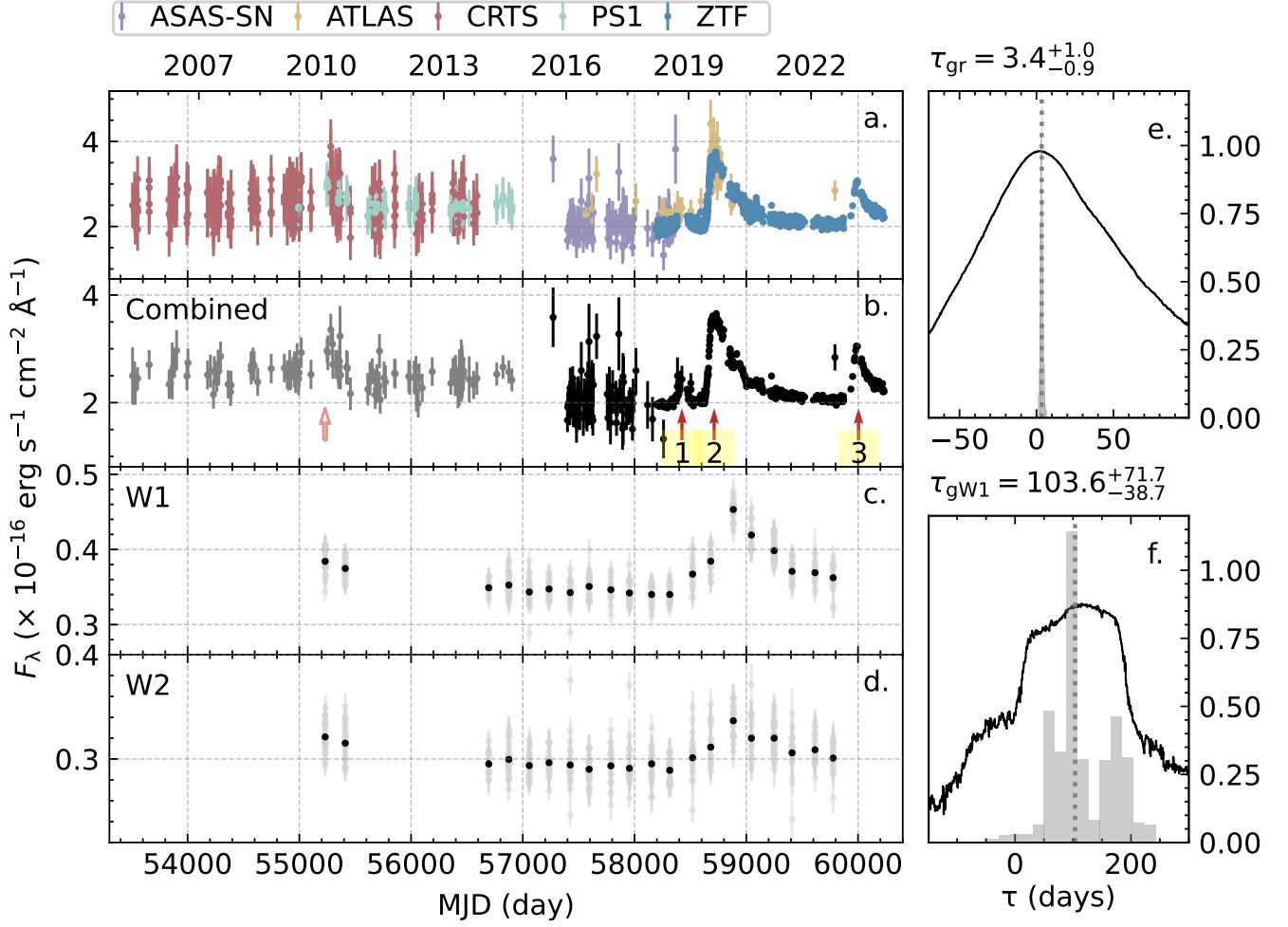


Figure 2. The archived light curves in observer frame and time lag measurements in rest frame for AT 2021aek. Panel a displays the flux-scaled photometry data, compiled from ZTF, ASAS-SN, ATLAS, CRTS, and PS1, each marked in different colors. Panel b shows the combined light curve within 2 days. The red-filled arrows with numbers mark three identified flares and the red unfilled arrow around MJD 55200 marks a potential flare. The grey data points are not flux-scaled with the black data points due to the sampling gap around MJD 57000 (see Sec.2.2). Panels c and d present *W1*- and *W2*-band photometric data from AllWISE and NEOWISE surveys in grey points, along with the weighted mean every six months marked in black. All fluxes are in the unit of 10^{-16} erg s^{-1} cm^{-2} \AA^{-1} . Panel e presents the ICCF between ZTF *g*- and *r*-band light curves and the centroid time lag $\tau_{g,r}$ is noted above Panel e. The grey histogram represents the distribution of the centroid lags obtained from the Monte-Carlo calculation. Panel f displays the CCF between the ZTF *g*-band and *WISE W1*-band. The analysis details can be found in Sec.3.1.2.

subsequent analysis since we focused on the light curves after MJD 57000. ATLAS and ASAS-SN present highly consistent variation with ZTF data, indicating the robustness of flux calibration.

We also compiled the mid-infrared *WISE* data (see Fig. 2) and obtained 20 binned (within 50 days) data points from 2010 to 2023 on *W1* ($3.4\mu\text{m}$) and *W2* ($4.6\mu\text{m}$) bands.

2.3. Spectra of AT 2021aek

The optical spectra (see Fig.3) were obtained by the Multiple Mirror Telescope (MMT) in 1997 (First Bright Quasar Survey, White et al. 2000) and the Sloan Digital Sky Survey (SDSS) in 2003. The spectra from MMT and SDSS are with the similar emission line features, but the minor

difference in flux level which may be caused by different fiber apertures or flux calibrations. The detection of BF lines (see grey shaded part in Fig.3), particularly N III $\lambda\lambda 4640$ (Bowen 1928; Netzer et al. 1985), is uncommon in typical AGN spectra (Vanden Berk et al. 2001). Their co-existence with strong He II in both MMT and SDSS spectra implies the presence of a powerful X-ray/UV photon source in AT 2021aek (Leloudas et al. 2019).

3. MEASUREMENT AND ANALYSIS

3.1. Light Curve Characterization

We present optical and infrared light curves in Fig.2. The optical light curves span approximately 16 years, with the

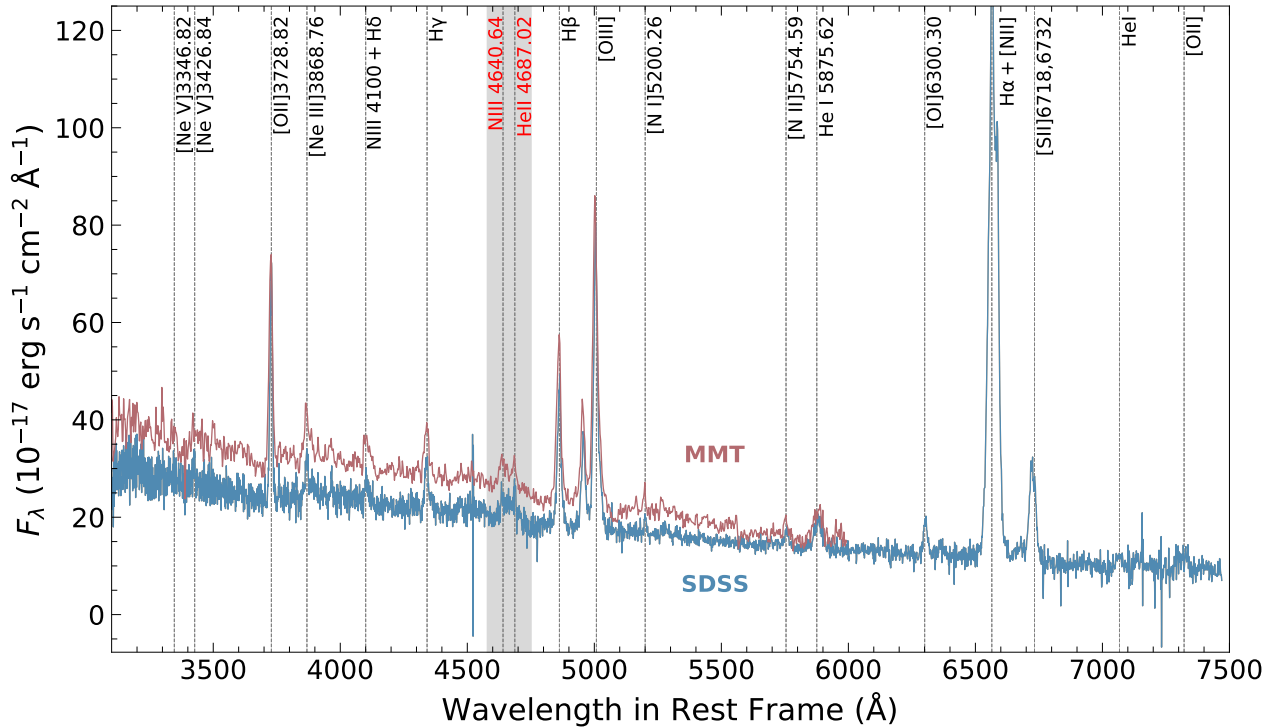


Figure 3. The archival spectra of J1612 from MMT (in 1997) and SDSS (in 2003). The dashed lines mark the prominent emission lines and the grey span marks the BF lines (also see Sec.4.4).

source remaining mostly quiescent, exhibiting no significant flux fluctuation for the majority of the time. While both CRTS and PS1 data suggest a possible rising feature around MJD 55200, limitations in data quality make it difficult to determine its validity. Therefore, we focus our analysis on the calibrated data after MJD 57000 for a more robust investigation of flares in AT 2021aek. In the past five years, AT 2021aek exhibited three optical flares (hereafter Flares I, II, and III respectively as noted in Fig.2) between Modified Julian Day (MJD) 58000 and 60400. Due to the discrepancy of data in the observational gap, the brightening feature around MJD 58,400 (Flare I) is ambiguous. Flare II exhibited rapid brightening and a slow power-law decline lasting ~ 1000 days (in rest frame) after the peak, followed by Flare III displaying milder brightening but a similar light curve pattern. The $g-r$ color evolution during the flaring is presented in Fig.4, in which the reference magnitudes were subtracted with $L_{v,0}$ obtained in Sec.3.1.1. The color exhibited rapid drop and quick recovery during Flare II followed by a minor evolution in blue colors.

The *WISE* light curves reveal a broad, intense flare around MJD 59000, coincident with Flare I and II seen in the optical light curve, suggesting a wide distribution of hot dust. Due to the lack of *WISE* data, the infrared echo to the Flare III around MJD 60000 remains unclear. The *W1-W2* color evolution during the flaring is presented in Fig.4, in which the *W1-W2* maintains above 0.8 mag, consistent with the AGN

criterion in Stern et al. (2012). The color generally shows minor evolution considering the scattering of original data sets (see grey points in Fig.2), and the drop around 530 days may be induced by measurement uncertainties.

The physical mechanism behind these flares remains unclear. In this section, we apply a generic quantitative analysis for TDEs to AT 2021aek to draw comparisons and explore the possible origins.

3.1.1. Light Curve Fitting

To quantify the rapid rise and slow decline in AT 2021aek’s light curves for Flares II and III, we adopt the fitting approach described by van Velzen et al. (2021). This method utilizes a combination of a Gaussian function for the rise phase and a power law for the decay phase, as given by the following equation,

$$L_{\nu}(t) = L_{\nu}^{\text{peak}} \times \begin{cases} e^{-(t-t_{\text{peak}})^2/2\sigma^2} & t \leq t_{\text{peak}} \\ \left(\frac{t-t_{\text{peak}}+t_0}{t_0}\right)^p & t > t_{\text{peak}} \end{cases} \quad (1)$$

where L_{ν} is the luminosity, and L_{ν}^{peak} is the peak luminosity at time t_{peak} .

The intrinsic variations of flares need to be isolated from the AGN and/or host galaxy contributions during the quiescent periods. However, the overlap of multiple flares on the light curve make this separation uncertain. We added

Parameters	Description	Priors	Units
$L_{\nu,0}$	Luminosity in Quiescent time	[1,4]	$10^{44} \text{erg s}^{-1}$
$\log L_{\nu}^{\text{peak}}$	Peak Luminosity	[0.01, 10]	$10^{44} \text{erg s}^{-1}$
t_{peak1}	Peak Time of Flare II	[20, 200]	days
t_{peak2}	Peak Time of Flare III	[1000, 1200]	days
p	Power-law Decay Index	[-10,0]	
$\log \sigma$	Gaussian Rise Time	[-3, 2]	days
$\log t_0$	Power-law Normalization	[-1, 5]	days

Table 1. Priors for MCMC Analysis. Except for t_{peak} , we adopted the same prior distributions for other parameters of Flare II and Flare III.

best-fit parameters at the peak luminosity are summarized in Table 3.

3.1.2. Time Lag Measurements

The time delay between UV-optical-near-Infrared light curves is characteristic evidence of AGN variability caused by reprocessing of radiation from the inner accretion disk at different radii by the corona (Krolik et al. 1991; Cackett et al. 2007, 2021). In the standard accretion disk model, the inter-band delay scales with wavelength as $\tau \propto \lambda^{4/3}$. For typical AGN variability, the predicted time delay can be estimated based on the black hole mass and luminosity, which is commonly ~ 2 -3 times smaller than the observed time delay (Fausnaugh et al. 2018; Kara et al. 2021; Guo et al. 2022). As such, UV-optical time lag measurement will help distinguish between intrinsic AGN variability and some other mechanism, such as TDEs, as the origins of flares in AT 2021aek.

The time spans (in rest frame) of ZTF g -band and r -band are over 1500 days and the mean sampling cadences are ~ 1.23 days and ~ 0.94 days. We use the interpolated cross-correlation function (ICCF; Gaskell et al. 1986; Peterson 1993) to measure the time delays in the rest frame (see Fig. 2). The centroid lags above 85% of the coefficient peak are adopted as final lags, and the uncertainties are estimated from Flux Randomization/Random Subset Sampling (FR/RSS) (Peterson et al. 1998). We obtained a reliable time lag of $\tau_{g,r} = 3.4^{+1.0}_{-0.9}$ days.

We also obtained an estimated time delay of $\tau_{g,W1} = 103.6^{+71.7}_{-38.7}$ days between the g -band and the *WISE-W1* light curve (Fig. 2, panel f). The mean sampling cadence is $\sim 146.85 \pm 13.39$ days, indicating the sample deficiency which may introduce uncertainties in the measurement of g -*W1* time lag.

3.2. Spectral Fitting and BH Properties

We employ DASpec³ to perform spectral decomposition on the SDSS spectrum and estimate black hole mass and accretion rate. The continuum is composed of a power-law AGN continuum, galaxy template, and Fe II pseudo-continuum. Emission lines were modeled with a single or double Gaussian depending on the line profiles. Double Gaussians were used for broader lines [O III] $\lambda\lambda$ 4959, 5007 potentially affected by outflows. The full-width at half maximum (FWHM) and line shift parameter are tied together to account for the common broadening mechanism. The flux ratio between H β and [O III] λ 5007 was fixed at the canonical value of 0.1 for NLSy1 fitting (Veilleux & Osterbrock 1987; Vaona et al. 2012; Huang et al. 2019). Similarly, the FWHM and line shift of the [N II] $\lambda\lambda$ 6548, 6583 and [S II] $\lambda\lambda$ 6716, 6730 doublets were tied together. Additional Gaussian components were used to describe the broad H β and H α emission arising from the broad line region (BLR).

Due to weak galaxy absorption features and Fe II pseudo-continuum, their contribution to the 5100 Å luminosity is negligible. We obtained a 5100 Å luminosity of $\log L_{5100} = 44.29 \pm 0.01 \text{ erg s}^{-1}$, and we estimated a BLR size of $\sim 47.80^{+5.22}_{-5.06}$ lt-days based on the R-L relationship from Bentz et al. 2013. We measured the FWHM of the broad H β ($1091 \pm 269 \text{ km s}^{-1}$) and H α ($1788 \pm 149 \text{ km s}^{-1}$) emission lines. Under the virial assumption, we obtained the BH mass (Blandford & McKee 1982; Peterson 1993),

$$M_{\bullet} = f_{\text{BLR}} \frac{R_{\text{BLR}} V^2}{G} \quad (3)$$

where $R_{\text{BLR}} = c\tau_{\text{BLR}}$ is the responsivity-weighted radius of the BLR, τ_{BLR} is the time lag, c is the speed of light, V is the FWHM of the emission lines from the spectra, G is the gravitational constant, and f_{BLR} is a scaling factor taken as 1.12 for NLSy1 (Woo et al. 2010). The BH masses estimated from H β and H α are $\log(M_{\bullet}) = 7.09^{+0.18}_{-0.31} M_{\odot}$ and $\log(M_{\bullet}) = 7.52^{+0.08}_{-0.10} M_{\odot}$, respectively. These masses generally agree with previous estimates for this source: $M_{\bullet} = 10^{7.3} M_{\odot}$ based on H α (Greene & Ho 2007) and $M_{\bullet} = 10^{6.8} M_{\odot}$ based on H β (Cracco et al. 2016). We also gave the estimation of dimensionless accretion rate (Frank et al. 2002; Netzer 2013; Wang et al. 2014),

$$\dot{M} = 20.1 \frac{\ell_{44}}{\cos i} m_7^{-3/2} \quad (4)$$

where $\ell_{44} = L_{5100}/10^{44} \text{ erg s}^{-1}$, and $m_7 = M_{\bullet}/10^7 M_{\odot}$. i is the inclination of the disk to the line of sight, and we take $\cos i = 0.75$ (Du et al. 2016). We obtain the accretion rate of ~ 1.74 and ~ 0.88 from BH masses derived from H β and H α , respectively. To assess the accretion power for the flares, we eliminate the intrinsic AGN and/or host galaxy contribution $L_{\nu,0}$ and calculated the Eddington ratio ($\lambda_{\text{Edd}} = L_{\text{bb}}^{\text{peak}}/L_{\text{Edd}}$) of ~ 0.58 and ~ 0.38 at the peak luminosity

³ <https://github.com/PuDu-Astro/DASpec>

Table 2. Best-Fitting Values for Light Curves.

Band	Flare	$L_{\nu,0}$ (10^{44} erg s $^{-1}$)	L_{ν}^{peak} (10^{44} erg s $^{-1}$)	t_{peak} (days)	σ (days)	t_0 (days)	p	$t_{1/2,\text{rise}}$ (days)	$t_{1/2,\text{decay}}$ (days)
(1)	(2)	(3)	(4)	(5)	(6)	(7)	(8)	(9)	(10)
g, r, i	I	2.27
	II	2.27	$2.07^{+0.01}_{-0.01}$	$82.86^{+0.38}_{-0.38}$	$24.98^{+0.26}_{-0.25}$	$455.40^{+26.75}_{-25.02}$	$-2.99^{+0.13}_{-0.14}$	$30.45^{+0.49}_{-0.49}$	$117.99^{+14.78}_{-13.30}$
	III	2.27	$1.19^{+0.03}_{-0.03}$	$1129.01^{+2.02}_{-1.91}$	$28.48^{+2.12}_{-1.98}$	$127.41^{+76.68}_{-38.73}$	$-1.61^{+0.34}_{-0.65}$	$33.97^{+3.95}_{-3.81}$	$79.41^{+78.37}_{-50.93}$
g	I	2.19
	II	2.19	$2.16^{+0.01}_{-0.01}$	$79.15^{+0.51}_{-0.49}$	$23.93^{+0.34}_{-0.33}$	$519.22^{+47.14}_{-39.66}$	$-3.37^{+0.20}_{-0.24}$	$28.18^{+0.91}_{-0.91}$	$118.67^{+23.23}_{-19.51}$
	III	2.19	$1.29^{+0.05}_{-0.05}$	$1129.32^{+3.48}_{-3.40}$	$27.49^{+4.42}_{-3.88}$	$161.08^{+147.54}_{-71.70}$	$-1.99^{+0.66}_{-1.30}$	$34.41^{+7.52}_{-6.78}$	$75.12^{+187.12}_{-62.95}$
r	I	2.27
	II	2.27	$2.16^{+0.02}_{-0.02}$	$85.76^{+0.67}_{-0.73}$	$26.61^{+0.42}_{-0.45}$	$345.79^{+23.84}_{-22.21}$	$-2.49^{+0.12}_{-0.13}$	$31.32^{+1.04}_{-1.05}$	$110.79^{+16.51}_{-14.61}$
	III	2.27	$1.15^{+0.04}_{-0.04}$	$1127.93^{+2.42}_{-2.42}$	$26.08^{+2.36}_{-2.12}$	$146.25^{+151.60}_{-58.21}$	$-1.73^{+0.49}_{-1.21}$	$33.53^{+4.25}_{-4.03}$	$86.15^{+203.74}_{-63.20}$
i	I	2.57
	II	2.57	$2.14^{+0.04}_{-0.04}$	$96.52^{+2.35}_{-2.25}$	$32.42^{+1.47}_{-1.52}$	$385.57^{+73.24}_{-53.96}$	$-2.30^{+0.25}_{-0.33}$	$38.17^{+3.46}_{-3.47}$	$135.78^{+56.26}_{-40.91}$
	III	2.57

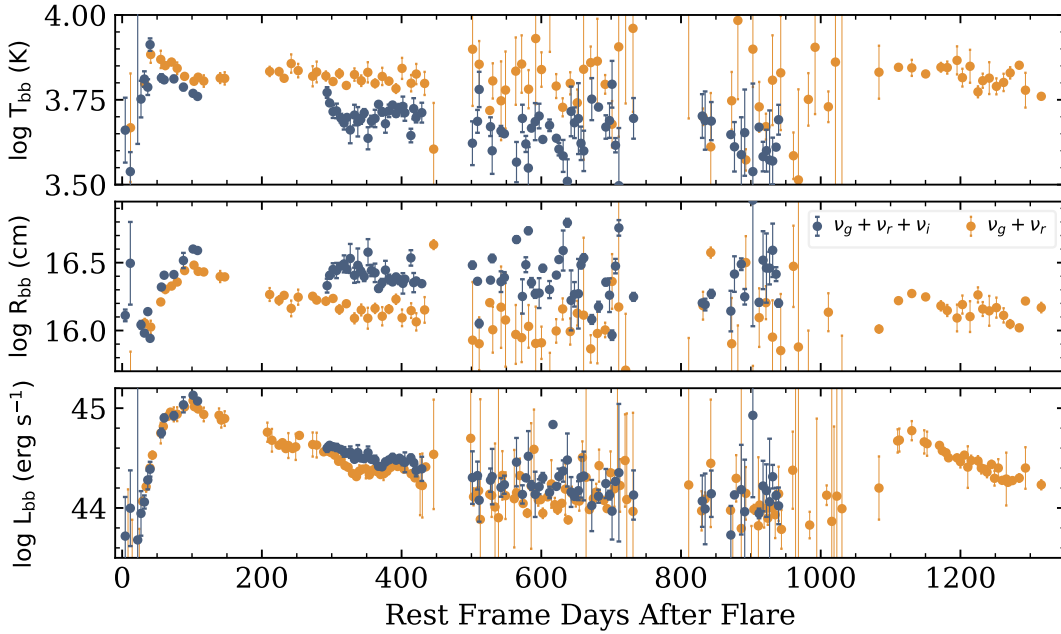


Figure 5. The blackbody temperature, radius, and luminosity for AT 2021aeuk in the top, middle, and bottom panels, respectively. The dark blue dots represent the results obtained from ZTF g -, r -, i -band data, while the orange dots correspond to the results derived from g -, r -band data. The x -axis is the same as Fig. 4.

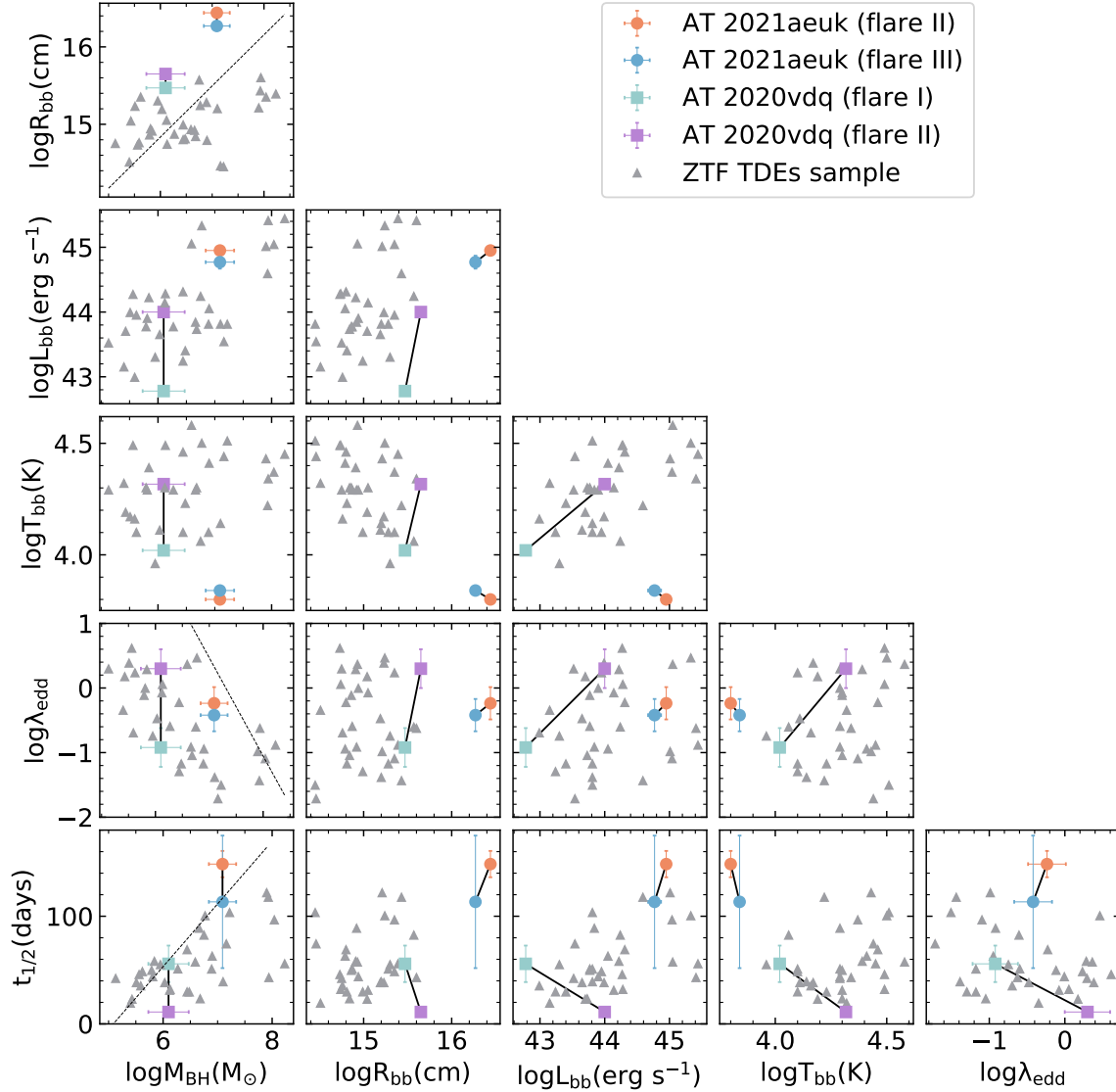


Figure 6. The physical parameters of ZTF TDEs and two flares in AT 2021aeuk and AT 2020vdq. The flares of AT 2021aeuk are represented by orange and blue dots, while the flares of AT 2020 vdq are represented by green and purple dots. The TDE samples from Yao et al. (2023) are presented in the grey dots. The grey dotted lines are the predicted scaling relationships $R_{\text{bb}} \propto M_{\bullet}^{2/3}$ for the fiducial cooling envelop model from Metzger & Stone (2016), and $\lambda_{\text{Edd}} \propto M_{\bullet}^{-3/2}$, and $t_{1/2} \propto M_{\bullet}^{1/2}$ (for the most tightly bound debris) from Stone et al. (2013), respectively.

Table 3. The physical parameters inferred from the light curve.

Flare	$\log L_{\text{bb}}^{\text{peak}}$ (erg s^{-1})	$\log T_{\text{bb}}^{\text{peak}}$ (K)	λ_{Edd}	$\log E_{\text{bb}}$ (erg)
(1)	(2)	(3)	(4)	(5)
I
II	$44.95^{+0.03}_{-0.03}$	$3.80^{+0.01}_{-0.01}$	0.58	52.30
III	$44.77^{+0.10}_{-0.10}$	$3.84^{+0.02}_{-0.02}$	0.38	52.07

of Flare II and III, where $L_{\text{Edd}} \equiv (M_{\text{BH}}/M_{\odot}) \times 1.25 \times 10^{38} \text{erg s}^{-1}$ (Yao et al. 2023). The results are presented in Table 3.

4. DISCUSSION

4.1. Scenario of Radio-Beaming Effect

The estimated occurrence rate of radio-loud AGNs among NLSy1 is $\sim 4\%$ (Komossa et al. 2006; Zhou et al. 2006; Rakshit et al. 2017; Singh & Chand 2018). J1612, as an NLSy1, is classified as a flat-spectrum radio quasar (FSRQ) with a loudness parameter of $\log R^* \sim 1.06$. The radio-loud nature and the VLA resolved features (Berton et al. 2018) of J1612 suggest the potential presence of relativistic jets. The jets are a hallmark of blazars, where the emission is Doppler-boosted due to the beaming effect along the jet direction. In J1612, the optical emission might be similarly influenced by this beaming effect. We explore the possibility of the radio-beaming effect contributing to the optical flares in AT 2021aeuk. However, based on the following evidence, we argue that jet-induced emission likely plays a minor role in the observed optical flares,

- **Light Curve Morphology.** Blazars are renowned for their highly variable optical emission, exhibiting rapid rise and fall times with a symmetrical light curve shape (Raiteri et al. 2003; Rani et al. 2010; Gopal-Krishna et al. 2011; Goyal et al. 2018). This behavior is distinct from the observed optical flares in AT 2021aeuk, which displayed a fast rise but a slow, monotonical decline.
- **Optical-Infrared Time Delay.** Blazars generally exhibit minimal time lags between their optical and near-Infrared emission variations, typically on the order of days or less (Paltani et al. 1997; Neugebauer & Matthews 1999; Raiteri et al. 2006; Bonning et al. 2012; Liao et al. 2019; Lyu et al. 2019; Perger et al. 2023). In contrast, the observed delay of about 120 days between the optical and g - WI ($3.4 \mu\text{m}$) flares in AT 2021aeuk (see Fig.2) is significantly longer than what can be explained by standard blazar infrared emission processes, which can instead be explained by the dust reprocessing from the dusty torus.
- **Long-Term Quiescent State.** The blazar state of FSRQs is considered to last for decades, with occasional state transitions on year-long timescales

(Chand & Gopal-Krishna 2022). However, the 16-year light curve suggests that AT 2021aeuk spends most of this period in a low state, exhibiting major flares only during recent years. Besides, we corrected the extinction of the SDSS photometry ($R_V = 3.1$, $E(B - V) = 0.014$, Fitzpatrick 1999) and yielded magnitudes of $r = 17.8$ and $g = 18.2$, which are consistent with the ZTF photometry obtained during the quiescent state.

- **Absence of γ -ray counterpart.** Blazars typically exhibit a strong correlation between optical and γ -ray emission variations, with γ -rays often leading the optical changes by a small time delay (e.g., Rani et al. 2013). Interestingly, no γ -ray counterpart was detected by the *Fermi* Large Area Telescope (LAT) during the flaring periods in AT 2021aeuk (private communication with Jun-Rong Liu). Although “orphan flares” have been observed in blazars, they only appear in one band (γ -ray band or optical band) and do not have counterparts in the other band. The mechanism can be the accretion-disk outbursts or stochastic fluctuation of multiple zones, but the orphan flares usually come with rather lower amplitudes (Liodakis et al. 2019).

4.2. Scenario of TDEs

Large-scale optical sky surveys have significantly boosted the number of discovered UV-optical TDEs. However, TDE identification remains challenging due to the uncertainties surrounding their physical origin and the relatively limited number of confirmed cases. Consequently, the current criteria for identifying TDEs are primarily based on observable features, and we investigate the criteria proposed by van Velzen et al. (2019, 2020) below. It should be noted that some TDEs exhibiting atypical characteristics which might not satisfy the established criteria.

- **Nuclear.** The observed infrared echo (see Sec.3.1.2 and Fig.2) indicates the thermal reprocessing of dusty torus ignited either by AGN accretion (Barvainis 1987) or nuclear transients, like supernova or TDE (Lu et al. 2016; Dou et al. 2017; Jiang et al. 2017; Yang et al. 2019). However, the observed time lag ($\sim 103.6^{+71.7}_{-38.7}$ days), while uncertain, is generally smaller than the expected light traveling time in the mid-infrared band (~ 325.0 days) induced by the typical AGN radiation with $\log L_{5100} = 44.29 \pm 0.01 \text{erg s}^{-1}$ (Koshida et al. 2014; Minezaki et al. 2019; Lyu et al. 2019; Chen et al. 2023a). This suggests that the distance between the UV/optical emitter and the dusty region is relatively smaller than the expected distance between the dusty torus and the accretion disk. The infrared echo is more likely induced by nuclear transients like TDE or supernova.
- **Spectroscopy** The spectra from MMT (1997) and SDSS (2003) (see Fig.3) are not taken during the flare. However, they both exhibited prominent N III $\lambda 4640$, which suggests the unusual local metallicity

abundance. A TDE with a high-mass star can be attributed to the abundance (e.g., Kochanek 2016; Liu et al. 2018), and the line width of N III $\lambda 4640$ and He II $\lambda 4686$ may be highly broadened through electron scattering during the flares (Roth & Kasen 2018; Leloudas et al. 2019). Since we do not have spectra during the flares, we cannot distinguish them from other physical mechanisms (as stated in Sec.4.4).

- **Light Curve Morphology.** Similar to typical TDE light curves, both Flare II and Flare III in AT 2021aek exhibit a rapid rise followed by a slower decline. The $t_{1/2, \text{rise}}$ for Flare II ($30.45^{+0.49}_{-0.49}$ days) and Flare III ($33.97^{+3.95}_{-3.81}$ days) are generally consistent and the $t_{1/2, \text{decay}}$ for Flare II ($117.99^{+14.78}_{-13.30}$ days) is longer than that for Flare III ($79.41^{+78.37}_{-50.93}$ days). However, during the decay phase, the power-law index for Flare II ($p = -2.99^{+0.13}_{-0.14}$) is steeper than the theoretical value of $-5/3$. On the other hand, Flare III's index ($p = -1.61^{+0.34}_{-0.65}$) falls closer to the expected value which may vary with new coming data afterward. Besides, Flare II and III exhibited post-peak bumps during the decay phase, which may be explained as the late-time forming of the disk during the TDE (Guo et al. 2023a).
- **Color and Temperature.** The $g - r$ color (see Fig.4) during the flare remains blue, and it exhibited a rapid drop and quick recovery during Flare II followed by minor evolution later, which are consistent with the behaviors of typical TDEs (van Velzen et al. 2021; Yao et al. 2023). The blackbody temperature (see Fig.5) from ZTF $g-$, $r-$ band fitting exhibited no significant cooling trend, which is consistent with the behaviors in most UV/optically-selected TDEs (van Velzen et al. 2021; Gezari 2021; Yao et al. 2023). The peak temperatures measured for Flare II ($\log T_{\text{bb}}^{\text{peak}} \sim 3.80^{+0.01}_{-0.01}$) and Flare III ($\log T_{\text{bb}}^{\text{peak}} \sim 3.84^{+0.02}_{-0.02}$) are significantly lower than the values typically observed in UV/optical TDEs ($> 1.2 \times 10^4 \text{K}$, see Fig.6, van Velzen et al. 2020; Yao et al. 2023). However, the lack of UV photometry and internal extinction correction may introduce some uncertainties in blackbody fitting. These behaviors also disfavor the SN origin which will show post-peak color reddening and prominent temperature cooling. It should be noted that the minor temperature post-peak drop may be induced by the peak variation inconsistency between ZTF $g-$, $r-$ bands (see Panels a and b in Fig.4).

The current analysis is insufficient for a definitive TDE classification based on the criteria discussed above. To gain further insights of the origin, we compared their disruption properties (see Fig.6) with those of well-established TDEs (Yao et al. 2023). The blackbody radius of AT 2021aek ($\gtrsim 10^{16}$ cm) is larger than it typically is in other TDEs. It also deviates from the predicted $R_{\text{bb}} \propto M_{\bullet}^{2/3}$ for the fiducial cooling envelope model (see Fig.6, Metzger & Stone 2016). The half-max during ($t_{1/2}$) is much longer than the typical

TDE samples. Interestingly, the event appears to follow the theoretical predictions (Stone et al. 2013) for $\lambda_{\text{Edd}} \propto M_{\bullet}^{-3/2}$ and $t_{1/2} \propto M_{\bullet}^{1/2}$.

4.3. Scenario of AGN Variation

- **Variability Pattern.** The typical AGN variability displays stochastically $\sim 10\%$ with symmetric flares and can be effectively produced by the damped random walk (DRW) model (Kelly et al. 2009; Kozłowski et al. 2010; MacLeod et al. 2010; Zu et al. 2013). Besides, the typical variation of NLSy1 is systematically smaller (Ai et al. 2010). Hence, the asymmetric flares of AT 2021aek, characterized by rapid smooth rise and slow decay, are unlikely well-described by the typical AGN variation.
- **Inter-band Time Lag.** The time lag of typical AGN variation between $g-$, $r-$ bands (see Sec.3.1.2) based on the standard disk model is $\tau_{g,r}^{\text{ss}} = 0.28$ days which is ~ 12.1 times shorter than the observed one ($\tau_{g,r} = 3.4^{+1.0}_{-0.9}$ in days). The substantially long delay is reported in some TDEs detected by ZTF (Guo et al. 2023b). Besides, the time lag between $g-$ and $WI-$ disfavors the typical AGN-induced torus echo (see Sec.4.2).

The asymmetric variation, the long $g-r$ time lag, and the short $g-WI$ time lag, and the distinct inter-band variation patterns all suggest that the physical mechanisms behind the optical flares in AT 2021aek are insufficient to be explained by a typical AGN radiation process.

The changing-state phenomenon in AGNs, where the broad emission lines emerge or go, can exhibit dramatic changes in optical brightness (typically months to years, Ricci & Trakhtenbrot 2023). This is commonly explained by the change in accretion rate caused by disk instabilities (Lin & Shields 1986; Balbus & Hawley 1991) or major disk perturbation (e.g., TDE, Merloni et al. 2015). Changing-state behaviors seem to prefer to reside in AGNs with low Eddington ratio with $\log L/L_{\text{Edd}} \lesssim -1.0$ (MacLeod et al. 2019; Green et al. 2022; Guo et al. 2024), which is smaller than the Eddington ratio of J1612 (~ 0.88 , see Sec.3.2). However, we do not have on-burst spectra and cannot verify whether the broad emission lines have gone through changing-look behaviors.

4.4. Scenario of Ambiguous Transients

The light curve evolution and pre-burst spectral properties of AT 2021aek exhibit notable deviations from the typical characteristics observed in most confirmed canonical transients induced by the single physical mechanism. We also compare AT 2021aek to several ambiguous transients (see Fig.7), including Bowen fluorescence flares (BFFs, Trakhtenbrot et al. 2019), ANTs/ENTs (Hinkle et al. 2024; Wiseman et al. 2024), and SLSNe-II (Miller et al. 2009; Gezari et al. 2009; Inserra et al. 2018). It is important to note that definitive classification remains challenging due to the limited number and the incomplete demography of these phenomena.

- **Light Curve Properties.** Flare II in AT 2021aek exhibits a prolonged decay phase (lasting over 1000 days). The blackbody temperature associated with Flare II/III is lower than typically seen in TDEs, additionally, the peak luminosity and blackbody radius are higher (see Fig.6). AT 2021loi, classified as a BFF (Makrygianni et al. 2023), also exhibited relatively low temperature and high released energy. Makrygianni et al. (2023) implies that the bumps during the decay might be the signature of BFF. Interestingly, Flare II and Flare III in AT 2021aek display the post-peak bumps which strengthens the possibility of AT 2021aek as a BFF.
- **Spectral Features.** The lack of on-burst spectra of AT 2021aek make it hard to to classify it among BFF, SLSN-II, or changing-look phenomenon. However, the pre-burst spectra of AT 2021aek exhibit prominent BF features, specifically broad He II $\lambda 4686$ and [N III] $\lambda 4640$, which suggest a vigorous or potentially long-lasting process that enriches the local metallicity. The presence of BF lines, uncommon in typical optical AGN spectra (Vanden Berk et al. 2001), suggests the excitation by intense extreme-ultraviolet (EUV) photons around 304Å (Osterbrock 1974). This raises the question of the origin of both the ionization source and the unusual metallicity abundance in these AGNs. Notably, nitrogen-loud quasars, identified in the UV band, are reported as a small fraction of typical AGNs (Osmer 1980; Jiang et al. 2008; Batra & Baldwin 2014), and the metallicity abundance can be attributed to the local star formation in the central region (Collin & Zahn 1999; Wang et al. 2011), the existence of Wolf-Rayet stars (Crowther 2007), TDE of a star going CNO cycle (Kochanek 2016; Liu et al. 2018; Leloudas et al. 2019; Blagorodnova et al. 2019; Neustadt et al. 2020; Malyali et al. 2021; Mockler et al. 2024), or enhancement/re-ignition of AGN accretion (Trakhtenbrot et al. 2019; Tadhunter et al. 2017; Blanchard et al. 2017; Gromadzki et al. 2019; Frederick et al. 2019; Makrygianni et al. 2023; Veres et al. 2024).
- **Multiple Flares.** Given the duration of the photometry data, it is challenging to determine whether the triple flares in AT 2021aek occur periodically. Flare III exhibited a lower energy release and Eddington ratio compared to Flare II (see Table.3). PS1-10adi showed weak recurring behavior, which Jiang et al. (2019) attributed to shock interactions between outflows and the torus. While AT 2021vdq (Somalwar et al. 2023), F01004-2237 (Veres et al. 2024; Sun et al. 2024) and AT2019aalc (Veres et al. 2024) exhibited recurring flares brighter than their initial outbursts, other transients, such as SN 2019meh (Soraisam et al. 2022) and AT 2021loi (Makrygianni et al. 2023), display sharp recurring flares during the decline phase. Interestingly, while the initial outburst of SN 2019meh is identified as an SLSN-

II (Nicholl et al. 2019), the subsequent flares exhibit sharp variations distinct from the post-peak bumps commonly explained by interactions with dense circumstellar material (Hosseinzadeh et al. 2022; Chen et al. 2023b). Additionally, the corresponding double-peak bump in the *WISE* light curve of SN 2019meh (although not explicitly shown in the relevant papers) further raises questions about the true nature of SN 2019meh.

4.5. Multiple Flares

While TDEs, SLSNe-II, or enhanced accretion process have been considered as potential explanations for flares in AT 2021aek, the physical mechanism responsible for the multiple occurrences remains uncertain. The flares can be considered as independent events with high occurrence rates under specific conditions. They can also be considered as recurring flares induced by the related physical process.

Galaxies with dense stellar environments, like Elliptical (E+A) galaxies with nuclear overdensities or post-starburst galaxies undergoing mergers, are favorable environments for a higher TDE rate (Arcavi et al. 2014; French et al. 2016; Stone & van Velzen 2016). Recent researches suggest that a luminous infrared galaxy (LIRG, Sanders et al. 1988; Hopkins et al. 2006), undergoing a late-stage merger event with intense star formation activity, might experience TDEs at a higher rate ranging from approximately $(1.6 - 4.6) \times 10^{-3} \text{ yr}^{-1} \text{ galaxy}^{-1}$ (Mattila et al. 2018; Kool et al. 2020; Reynolds et al. 2022). The Subaru image (see Fig.1) of J1612 reveals the minor tidal signatures and Berton et al. (2018) report a somewhat extended radio continuum. It also exhibits red mid-infrared color ($W1 - W2 = 1.1$). Barrows et al. (2021) analyzed the multi-wavelength spectral energy distribution (SED) of J1612 using data from GALEX, SDSS DR14, Gaia DR2, PanSTARR2, and 2MASS. Their analysis suggests a star formation rate (SFR) of approximately $6.6 M_{\odot} \text{ yr}^{-1}$ and a stellar mass of $5.4 \times 10^{10} M_{\odot}$ after separating the AGN contribution using CIGALE. We also give an SFR estimation of $7.0 M_{\odot} \text{ yr}^{-1}$ from emission lines [O II] and [O III] (Zhuang & Ho 2020), which is generally consistent with the SFR derived from SED fitting. However, the broadening of the [O III] line introduces some uncertainties into this measurement, and the SFR derived from SED fitting provides a more reliable estimate. These SFR values suggest that J1612 is unlikely to be classified as an LIRG. Notably, many AGN-associated transients display spectral features consistent with the NLSy1 galaxy, and J1612 was identified as an NLSy1 before the bursts. Frederick et al. (2021) proposed that NLSy1 galaxies might be particularly favorable environments for enhanced flare activity due to the instabilities of high accretion rate BHs. They also point out that it might be a selection effect for galaxies with low-mass BHs or ignorance of the smooth flares in broad-line AGNs.

A partial TDE (pTDE), where a stellar core survives and gravitationally interacts with the debris stream (Payne et al. 2021; Wevers et al. 2023; Malyali et al. 2023; Liu et al. 2023; Somalwar et al. 2023), can produce multiple flares

due to the ongoing interaction. This could be a contributing factor to the multiple flares in AT 2021aek. The models (Guillochon & Ramirez-Ruiz 2013; MacLeod et al. 2013; Mainetti et al. 2017; Coughlin & Nixon 2019; Miles et al. 2020) also predict a steeper index $p \sim -9/4$, which can be a possible explanation for index p deviation of Flare II in Sec.4.2, although we plotted the location for a pTDE, AT 2020vdq (Charalampopoulos et al. 2023; Somalwar et al. 2023; Yao et al. 2023), in Fig.6, and did not find much resemblance between it and AT 2021aek. ASSASN-14ko is a periodic pTDE candidate (Payne et al. 2021) with a mean recurring period of 114 ± 0.4 days. We did not examine the periodicity based on three flares in AT 2021aek, however, the partial disruption reduces the stellar mass and hence can alter the returning orbital period (Zhong et al. 2022). Further investigations with more pTDEs could provide valuable insights into the possibility of the origin of AT 2021aek.

Chan et al. (2019, 2020, 2021) carried out a series of simulations toward the interaction between TDE and accretion disk, where the debris stream punches through the disk, collides, and generates shocks causing disk material inflow. The TDE dynamics and disk mass distribution are altered, and the optical variation may not be a simple sum of the intrinsic AGN variability and the additional emission from the TDE. They predicted a power-law decay index between -3 and -2 early and potentially steeper later. The index p of Flare II ($-2.99^{+0.13}_{-0.14}$) is generally consistent with the prediction at the earlier time. They also predicted that the luminosity can reach a plateau due to the radiation trapping, where the inflow is faster than radiation diffusion. Interestingly, Flare II in AT 2021aek exhibits a plateau-like feature lasting for about 50 days in the g-band light curve (see Panel a in Fig. 4). For J1612 with BH mass $\sim 10^{7.52} M_{\odot}$ and Eddington ratio ~ 0.88 (if taking the $H\alpha$ case), it requires a disrupted star with rather high mass. They also predicted a “second impact” after the stream punched through the disk. The luminosity in X-ray or γ -ray follows the mass-return rate but in optical/UV it does not. Thus, this cannot sufficiently explain the subsequent Flare III.

Another intriguing hypothesis suggests that the triple flares observed in AT 2021aek might be a result of a stellar binary being disrupted by an SMBH binary (Wu & Yuan 2018). The interaction between the stellar binary and the SMBH binary can lead to multiple TDEs with varying time separations, influenced by the BH mass ratio, star masses, etc. For a stellar binary with two stars of $1 M_{\odot}$ each and a semi-major axis less than 100 AU, the time separation between flares in an SMBH binary system can range from 150 days to 15 years. In contrast, the time separation in a single SMBH system is generally much shorter. This model offers a potential explanation for the observed separation of over 1000 days between Flare II and Flare III in AT 2021aek. Furthermore, the binary black hole scenario aligns with the merging features observed in J1612, as captured by Subaru imaging.

5. SUMMARY

We report a rare transient AT 2021aek in a radio-loud NLSy1 galaxy (SDSS J161259.82+421940.3), with triple flares occurring between 2018 and 2023. We present archived photometry data from optical and infrared surveys, and then perform quantitative analysis based on the optical light curves and conduct spectral decomposition on the pre-burst spectra. The results are as follows,

- Despite the strong degeneracy between p and t_0 , the power-law decay index of Flare II ($p = -2.99^{+0.13}_{-0.14}$) is rather smooth compared to the current TDE sample, while Flare III's ($-1.61^{+0.34}_{-0.65}$) is generally consistent with the theoretical $-5/3$.
- The blackbody temperature shows minor evolution of $\sim 10^{3.8}$ K, much lower than the TDE sample. The $t_{1/2}$, blackbody radius ($\gtrsim 10^{16}$ cm) and released energy $\sim 10^{52}$ erg are generally larger.
- The time lag ($3.4^{+1.0}_{-0.9}$ days) between g - and r -bands is significantly larger (~ 12.1 times) than that from standard accretion disk prediction, and the peak variation of g - and r - band displays a different pattern. This indicates that the flares cannot solely be attributed to the typical AGN accretion process.
- The time lag ($103.6^{+71.7}_{-38.7}$) between g - and $W1$ -bands is significantly smaller than the value from $R - L$ prediction (~ 325 days). However, the sampling deficiency of the mid-infrared light curve introduces some uncertainties.
- The two pre-burst spectra show BF lines of [N III] $\lambda 4640$ indicating a vigorous or potentially long-lasting process that enriches the local metallicity. We derived a BH mass $\log M_{\bullet} = 7.09^{+0.18}_{-0.31} M_{\odot}$ and $\log M_{\bullet} = 7.52^{+0.08}_{-0.10} M_{\odot}$ using the FWHM of $H\beta$ and $H\alpha$ from spectral fitting, respectively, which are generally consistent with previous measurements. The corresponding AGN accretion rate is ~ 1.74 and ~ 0.88 .
- The Eddington ratio at peak luminosity of Flare II and III are ~ 0.58 and ~ 0.38 .

We compare AT 2021aek with blazars, TDEs, typical AGN intrinsic variation, SLSNe-II, and ambiguous flares. The possibility of blazars, typical AGN intrinsic variation, and SLSNe-II can be excluded based on the variation patterns, time delay, and recurring flares. AT 2021aek exhibited similar evolving patterns to TDEs. However, the long-term decay and the deviating blackbody parameters raise questions about TDE origin. The unconventional behaviors may induced by the coupling process between transients and accretion disk. The multiple flares can be explained as independent events with high occurrence in

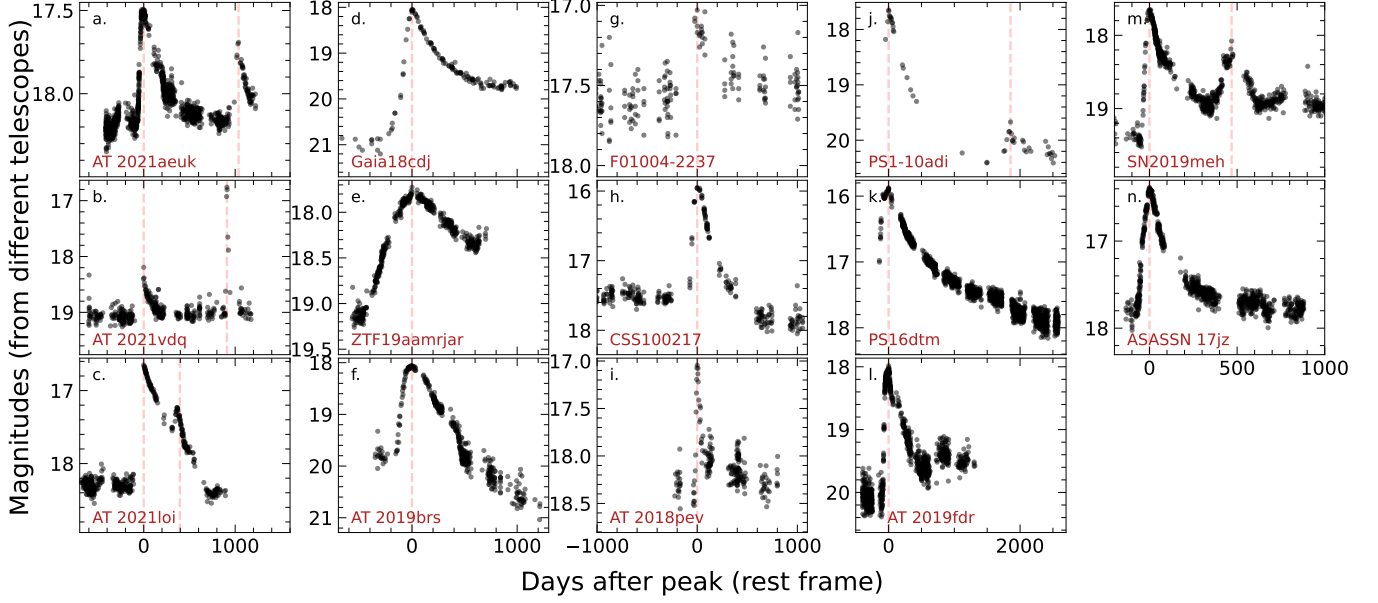


Figure 7. Long-term flares in the rest-frame day since flare. Panel a. is ZTF g -band data for AT 2021aeuk in this paper. Panel b. is ZTF g -band data for AT 2021vdq (pTDE candidate in Yao et al. 2023; Somalwar et al. 2023); Panel c. is ZTF g -band data for AT 2021loi (BFF candidate in Makrygianni et al. 2023); Panel d. is data for Gaia18cdj from Gaia Alert Transient Stream (ENT, TDE candidate in Hinkle et al. 2024); Panel e. is ZTF g -band data for ZTF19aamrjar (ANT in Wiseman et al. 2024); Panel f. is ZTF g -band data for AT 2019brs (BFF candidate in Frederick et al. 2021); Panel g. is V-band data from CRTS for F01004-2237 (TDE candidate in Tadhunter et al. 2017, BFF candidate in Trakhtenbrot et al. 2019); Panel h. is V-band data from CRTS for CSS100217 (SN II candidate in Drake et al. 2011, TDE candidate in Cannizzaro et al. 2022); Panel i. is ZTF g -band data for AT 2018pev (BFF candidate in Frederick et al. 2021); Panel j. is V-band data for PS1-10adi (SLSN-II or TDE candidate in Kankare et al. 2017; Jiang et al. 2019); Panel k. is Pan-STARRS data for PS16dtm (TDE candidate in Blanchard et al. 2017); Panel l. is ZTF g -band data for AT 2019fdr (TDE candidate in Frederick et al. 2021); Panel m. is ZTF g -band data for SN 2019meh (SLSN-II candidate in Nicholl et al. 2019; Soraisam et al. 2022); Panel n. is ATLAS data for ASASSN-17jz (SN II candidate in Holoien et al. 2022.)

certain environments. It can also be explained as recurring flares induced by the related physical processes. Multi-wavelength follow-up observations will be beneficial in determining the underlying physical mechanism responsible for AT 2021aeuk.

ACKNOWLEDGEMENTS

We really appreciate the referee for many precious comments that significantly improved the manuscript. Dong-Wei Bao and Wei-Jian Guo contributed equally to this work. We thank Hong Wu for using the Xinglong 2.16 m telescope to take a tentative spectrum of J1612 and Yu-Yang Songsheng for valuable discussions. We thank James Wicker for the invaluable help with polishing the language and correcting the language issues. We thank for Jun-Rong Liu’s *Fermi*-LAT data reduction and useful talk. We thank for Heng-Xiao Guo’s precious communication. This work was supported by National Science Foundation of China No. 11988101, 11973051. We acknowledge the support from the National Key R&D Program of China (2020YFC2201400, 2021YFA1600404), National Natural Science Foundation of China (NSFC-11991050, -11991054, -11833008, -12103041, -12263003, -12333003), the International Partnership Program of the Chinese Academy of Sciences (113111KYSB20200014)

and the science research grants from the China Manned Space Project with NO. CMS-CSST-2021-A05. W. Guo and H. Zou acknowledge the supports from National Key R&D Program of China (grant Nos. 2023YFA1607800, 2022YFA1602902, 2023YFA1608100, 2023YFF0714800, and 2023YFA1608303), the National Natural Science Foundation of China (NSFC; grant Nos. 12120101003, 12373010, 12233008, and 12173051), Beijing Municipal Natural Science Foundation (grant No. 1222028), and the science research grants from the China Manned Space Project with Nos. CMS-CSST-2021-A02 and CMS-CSST-2021-A04. YFY is supported by the Strategic Priority Research Program of the Chinese Academy of Sciences, Grant No. XDB0550200 and National SKA Program of China No. 2020SKA0120300. YRL acknowledges financial support from the NSFC through grant No 12273041 and from the Youth Innovation Promotion Association CAS. C.C. is supported by the National Natural Science Foundation of China, No. 11803044, 11933003, 12173045. This work is sponsored (in part) by the Chinese Academy of Sciences (CAS), through a grant to the CAS South America Center for Astronomy (CASSACA).

We also acknowledge SDSS for providing extensive spectral database support. SDSS is managed by the Astrophysical Research Consortium for the Participating

Institutions of the SDSS Collaboration including the Brazilian Participation Group, the Carnegie Institution for Science, Carnegie Mellon University, Center for Astrophysics — Harvard & Smithsonian, the Chilean Participation Group, the French Participation Group, Instituto de Astrofísica de Canarias, The Johns Hopkins University, Kavli Institute for the Physics and Mathematics of the Universe(IPMU)/University of Tokyo, the Korean Participation Group, Lawrence Berkeley National Laboratory, Leibniz Institut für Astrophysik Potsdam (AIP), Max-Planck-Institut für Astronomie (MPIA Heidelberg), Max-Planck-Institut für Astrophysik (MPA Garching), Max-Planck-Institut für Extraterrestrische Physik (MPE), National Astronomical Observatories of China, New Mexico State University, New York University, University of Notre Dame, Observatório Nacional/MCTI, The Ohio State University, Pennsylvania State University, Shanghai Astronomical Observatory, United Kingdom Participation Group, Universidad Nacional Autónoma de México, University of Arizona, University of Colorado Boulder, University of Oxford, University of Portsmouth, University of Utah, University of Virginia, University of Washington, University of Wisconsin, Vanderbilt University, and Yale University.

We acknowledge the efforts for public data from CTRS, PS1, ASAS-SN and ZTF. The Catalina Sky Survey is funded by the National Aeronautics and Space Administration under Grant No. NNG05GF22G issued through the Science Mission Directorate Near-Earth Objects Observations Program. The CRTS survey is supported by the US National Science Foundation under grants AST-0909182 and AST-1313422. The CRTS survey is supported by the US National Science Foundation under grants AST-0909182 and AST-1313422.

The PS1 has been made possible through contributions by the Institute for Astronomy, the University of Hawaii, the Pan-STARRS Project Office, the Max-Planck Society and its participating institutes, the Max Planck Institute for Astronomy, Heidelberg and the Max Planck Institute for Extraterrestrial Physics, Garching, The Johns Hopkins University, Durham University, the University of Edinburgh, Queen's University Belfast, the Harvard-Smithsonian Center for Astrophysics, the Las Cumbres Observatory Global Telescope Network Incorporated, the National Central University of Taiwan, the Space Telescope Science Institute, the National Aeronautics and Space Administration under Grant No. NNX08AR22G issued through the Planetary Science Division of the NASA Science Mission Directorate, the National Science Foundation under Grant No. AST-1238877, the University of Maryland, and Eotvos Lorand University (ELTE).

ASAS-SN is supported by the Gordon and Betty Moore Foundation through grant GBMF5490 to the Ohio State University and NSF grant AST-1515927. Development of ASAS-SN has been supported by NSF grant AST-0908816, the Mt. Cuba Astronomical Foundation, the Center for Cosmology and Astro- Particle Physics at the Ohio State

University, the Chinese Academy of Sciences South America Center for Astronomy (CASSACA), the Villum Foundation, and George Skestos.

ZTF is supported by the National Science Foundation under Grant No. AST-2034437 and a collaboration including Caltech, IPAC, the Weizmann Institute for Science, the Oskar Klein Center at Stockholm University, the University of Maryland, Deutsches Elektronen-Synchrotron and Humboldt University, the TANGO Consortium of Taiwan, the University of Wisconsin at Milwaukee, Trinity College Dublin, Lawrence Livermore National Laboratories, and IN2P3, France. Operations are conducted by COO, IPAC, and UW.

This publication makes use of data products from *WISE*, which is a joint project of the University of California, Los Angeles, and the Jet Propulsion Laboratory/California Institute of Technology, funded by the National Aeronautics and Space Administration. This publication also makes use of data products from *NEOWISE*, which is a project of the Jet Propulsion Laboratory/California Institute of Technology, funded by the Planetary Science Division of the National Aeronautics and Space Administration.

APPENDIX

A. APPENDIX FIGURE

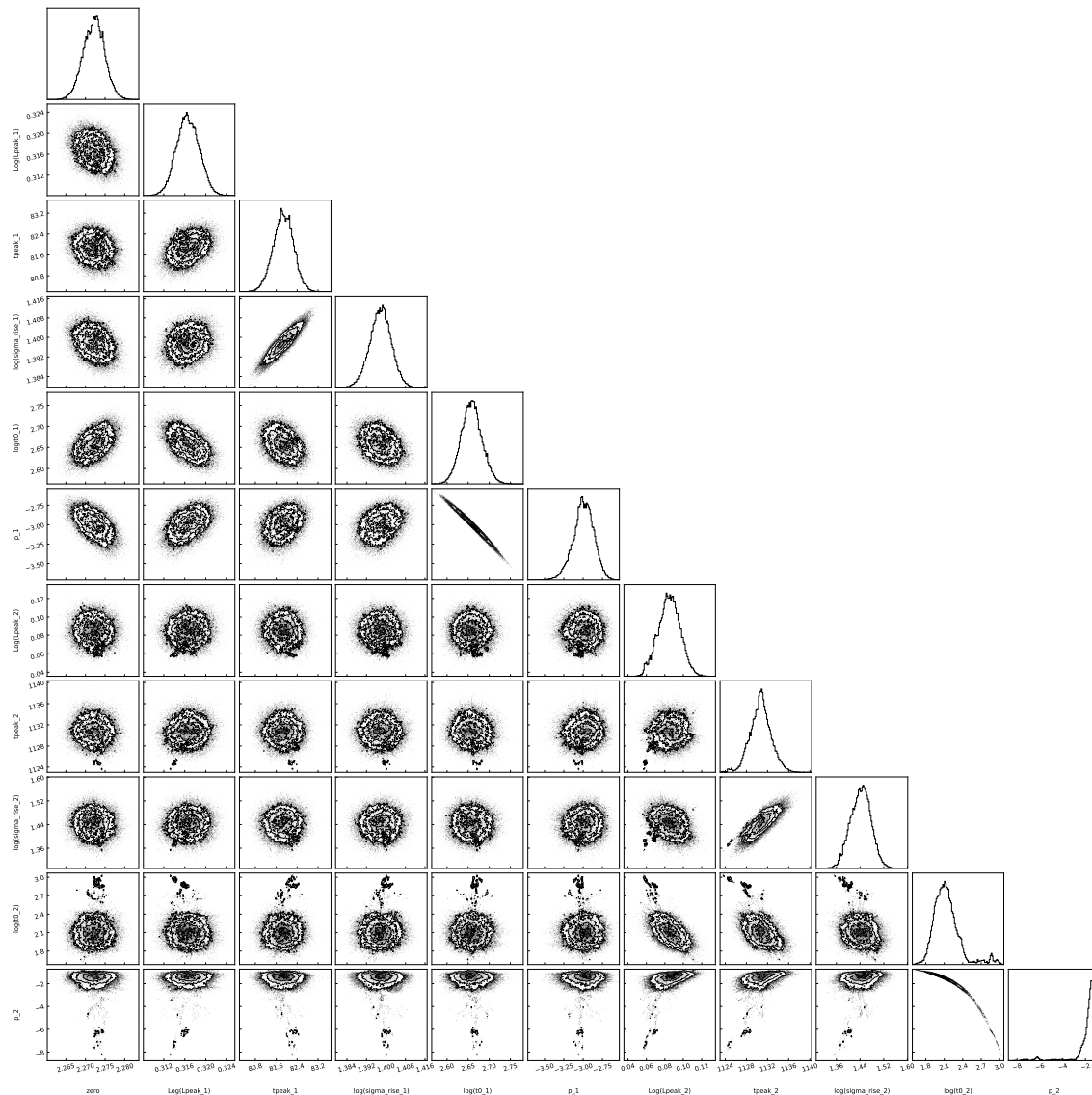


Figure A1. The MCMC posterior distributions of L_0 , L_V^{peak} , t_{peak} , σ , t_0 and p for Flare II and Flare III in Sec.3.1.1. The contours are at 1σ , 1.5σ , and 2σ levels. Note that t_{peak} , σ and t_0 are in the rest frame.

REFERENCES

- Ai, Y. L., Yuan, W., Zhou, H. Y., et al. 2010, *ApJL*, 716, L31, doi: [10.1088/2041-8205/716/1/L31](https://doi.org/10.1088/2041-8205/716/1/L31)
- Aihara, H., AlSayyad, Y., Ando, M., et al. 2022, *PASJ*, 74, 247, doi: [10.1093/pasj/psab122](https://doi.org/10.1093/pasj/psab122)
- Araudo, A. T., Bosch-Ramon, V., & Romero, G. E. 2010, *A&A*, 522, A97, doi: [10.1051/0004-6361/201014660](https://doi.org/10.1051/0004-6361/201014660)
- Arcavi, I., Gal-Yam, A., Sullivan, M., et al. 2014, *ApJ*, 793, 38, doi: [10.1088/0004-637X/793/1/38](https://doi.org/10.1088/0004-637X/793/1/38)

- Balbus, S. A., & Hawley, J. F. 1991, *ApJ*, 376, 214, doi: [10.1086/170270](https://doi.org/10.1086/170270)
- Barrows, R. S., Comerford, J. M., Stern, D., & Assef, R. J. 2021, *ApJ*, 922, 179, doi: [10.3847/1538-4357/ac1352](https://doi.org/10.3847/1538-4357/ac1352)
- Barvainis, R. 1987, *ApJ*, 320, 537, doi: [10.1086/165571](https://doi.org/10.1086/165571)
- Batra, N. D., & Baldwin, J. A. 2014, *MNRAS*, 439, 771, doi: [10.1093/mnras/stu007](https://doi.org/10.1093/mnras/stu007)
- Bentz, M. C., Denney, K. D., Grier, C. J., et al. 2013, *ApJ*, 767, 149, doi: [10.1088/0004-637X/767/2/149](https://doi.org/10.1088/0004-637X/767/2/149)
- Berton, M., Congiu, E., Järvelä, E., et al. 2018, *A&A*, 614, A87, doi: [10.1051/0004-6361/201832612](https://doi.org/10.1051/0004-6361/201832612)
- Blagorodnova, N., Cenko, S. B., Kulkarni, S. R., et al. 2019, *ApJ*, 873, 92, doi: [10.3847/1538-4357/ab04b0](https://doi.org/10.3847/1538-4357/ab04b0)
- Blanchard, P. K., Nicholl, M., Berger, E., et al. 2017, *ApJ*, 843, 106, doi: [10.3847/1538-4357/aa77f7](https://doi.org/10.3847/1538-4357/aa77f7)
- Blandford, R. D., & McKee, C. F. 1982, *ApJ*, 255, 419, doi: [10.1086/159843](https://doi.org/10.1086/159843)
- Bonning, E., Urry, C. M., Bailyn, C., et al. 2012, *ApJ*, 756, 13, doi: [10.1088/0004-637X/756/1/13](https://doi.org/10.1088/0004-637X/756/1/13)
- Böttcher, M. 2019, *Galaxies*, 7, 20, doi: [10.3390/galaxies7010020](https://doi.org/10.3390/galaxies7010020)
- Bowen, I. S. 1928, *ApJ*, 67, 1, doi: [10.1086/143091](https://doi.org/10.1086/143091)
- Cackett, E. M., Bentz, M. C., & Kara, E. 2021, *iScience*, 24, 102557, doi: [10.1016/j.isci.2021.102557](https://doi.org/10.1016/j.isci.2021.102557)
- Cackett, E. M., Horne, K., & Winkler, H. 2007, *MNRAS*, 380, 669, doi: [10.1111/j.1365-2966.2007.12098.x](https://doi.org/10.1111/j.1365-2966.2007.12098.x)
- Cannizzaro, G., Levan, A. J., van Velzen, S., & Brown, G. 2022, *MNRAS*, 516, 529, doi: [10.1093/mnras/stac2014](https://doi.org/10.1093/mnras/stac2014)
- Chambers, K. C., Magnier, E. A., Metcalfe, N., et al. 2016, arXiv e-prints, arXiv:1612.05560, doi: [10.48550/arXiv.1612.05560](https://doi.org/10.48550/arXiv.1612.05560)
- Chan, C.-H., Piran, T., & Krolik, J. H. 2020, *ApJ*, 903, 17, doi: [10.3847/1538-4357/abb776](https://doi.org/10.3847/1538-4357/abb776)
- . 2021, *ApJ*, 914, 107, doi: [10.3847/1538-4357/abf0a7](https://doi.org/10.3847/1538-4357/abf0a7)
- Chan, C.-H., Piran, T., Krolik, J. H., & Saban, D. 2019, *ApJ*, 881, 113, doi: [10.3847/1538-4357/ab2b40](https://doi.org/10.3847/1538-4357/ab2b40)
- Chand, K., & Gopal-Krishna. 2022, *MNRAS*, 516, L18, doi: [10.1093/mnras/slac066](https://doi.org/10.1093/mnras/slac066)
- Charalampopoulos, P., Leloudas, G., Pursiainen, M., & Kotak, R. 2023, *Transient Name Server AstroNote*, 115, 1
- Chen, Y.-J., Liu, J.-R., Zhai, S., et al. 2023a, *MNRAS*, 522, 3439, doi: [10.1093/mnras/stad1136](https://doi.org/10.1093/mnras/stad1136)
- Chen, Z. H., Yan, L., Kangas, T., et al. 2023b, *ApJ*, 943, 42, doi: [10.3847/1538-4357/aca162](https://doi.org/10.3847/1538-4357/aca162)
- Collin, S., & Zahn, J.-P. 1999, *A&A*, 344, 433
- Coughlin, E. R., & Nixon, C. J. 2019, *ApJL*, 883, L17, doi: [10.3847/2041-8213/ab412d](https://doi.org/10.3847/2041-8213/ab412d)
- Cracco, V., Ciroi, S., Berton, M., et al. 2016, *MNRAS*, 462, 1256, doi: [10.1093/mnras/stw1689](https://doi.org/10.1093/mnras/stw1689)
- Crowther, P. A. 2007, *ARA&A*, 45, 177, doi: [10.1146/annurev.astro.45.051806.110615](https://doi.org/10.1146/annurev.astro.45.051806.110615)
- Dgany, Y., Arcavi, I., Makrygianni, L., Pellegrino, C., & Howell, D. A. 2023, *ApJ*, 957, 57, doi: [10.3847/1538-4357/ace971](https://doi.org/10.3847/1538-4357/ace971)
- Dong, S., Chen, P., Bose, S., et al. 2016, *The Astronomer's Telegram*, 9843, 1
- Dou, L., Wang, T., Yan, L., et al. 2017, *ApJL*, 841, L8, doi: [10.3847/2041-8213/aa7130](https://doi.org/10.3847/2041-8213/aa7130)
- Drake, A. J., Djorgovski, S. G., Mahabal, A., et al. 2009, *ApJ*, 696, 870, doi: [10.1088/0004-637X/696/1/870](https://doi.org/10.1088/0004-637X/696/1/870)
- . 2011, *ApJ*, 735, 106, doi: [10.1088/0004-637X/735/2/106](https://doi.org/10.1088/0004-637X/735/2/106)
- Du, P., Lu, K.-X., Zhang, Z.-X., et al. 2016, *ApJ*, 825, 126, doi: [10.3847/0004-637X/825/2/126](https://doi.org/10.3847/0004-637X/825/2/126)
- Evans, C. R., & Kochanek, C. S. 1989, *ApJL*, 346, L13, doi: [10.1086/185567](https://doi.org/10.1086/185567)
- Fausnaugh, M. M., Starkey, D. A., Horne, K., et al. 2018, *ApJ*, 854, 107, doi: [10.3847/1538-4357/aaa2b](https://doi.org/10.3847/1538-4357/aaa2b)
- Fitzpatrick, E. L. 1999, *PASP*, 111, 63, doi: [10.1086/316293](https://doi.org/10.1086/316293)
- Foreman-Mackey, D., Hogg, D. W., Lang, D., & Goodman, J. 2013, *PASP*, 125, 306, doi: [10.1086/670067](https://doi.org/10.1086/670067)
- Frank, J., King, A., & Raine, D. J. 2002, *Accretion Power in Astrophysics: Third Edition*
- Frederick, S., Gezari, S., Graham, M. J., et al. 2019, *ApJ*, 883, 31, doi: [10.3847/1538-4357/ab3a38](https://doi.org/10.3847/1538-4357/ab3a38)
- . 2021, *ApJ*, 920, 56, doi: [10.3847/1538-4357/ac110f](https://doi.org/10.3847/1538-4357/ac110f)
- French, K. D., Arcavi, I., & Zabludoff, A. 2016, *ApJL*, 818, L21, doi: [10.3847/2041-8205/818/1/L21](https://doi.org/10.3847/2041-8205/818/1/L21)
- Gaskell, C. M., Cappellaro, E., Dinerstein, H. L., et al. 1986, *ApJL*, 306, L77, doi: [10.1086/184709](https://doi.org/10.1086/184709)
- Gezari, S. 2012, in *European Physical Journal Web of Conferences*, Vol. 39, European Physical Journal Web of Conferences, 03001, doi: [10.1051/epjconf/20123903001](https://doi.org/10.1051/epjconf/20123903001)
- Gezari, S. 2021, *ARA&A*, 59, 21, doi: [10.1146/annurev-astro-111720-030029](https://doi.org/10.1146/annurev-astro-111720-030029)
- Gezari, S., Halpern, J. P., Grupe, D., et al. 2009, *ApJ*, 690, 1313, doi: [10.1088/0004-637X/690/2/1313](https://doi.org/10.1088/0004-637X/690/2/1313)
- Gopal-Krishna, Goyal, A., Joshi, S., et al. 2011, *MNRAS*, 416, 101, doi: [10.1111/j.1365-2966.2011.19014.x](https://doi.org/10.1111/j.1365-2966.2011.19014.x)
- Goyal, A., Stawarz, Ł., Zola, S., et al. 2018, *ApJ*, 863, 175, doi: [10.3847/1538-4357/aad2de](https://doi.org/10.3847/1538-4357/aad2de)
- Green, P. J., Pulgarin-Duque, L., Anderson, S. F., et al. 2022, *ApJ*, 933, 180, doi: [10.3847/1538-4357/ac743f](https://doi.org/10.3847/1538-4357/ac743f)
- Greene, J. E., & Ho, L. C. 2007, *ApJ*, 667, 131, doi: [10.1086/520497](https://doi.org/10.1086/520497)
- Gromadzki, M., Hamanowicz, A., Wyrzykowski, L., et al. 2019, *A&A*, 622, L2, doi: [10.1051/0004-6361/201833682](https://doi.org/10.1051/0004-6361/201833682)
- Guillochon, J., Manukian, H., & Ramirez-Ruiz, E. 2014, *ApJ*, 783, 23, doi: [10.1088/0004-637X/783/1/23](https://doi.org/10.1088/0004-637X/783/1/23)
- Guillochon, J., & Ramirez-Ruiz, E. 2013, *ApJ*, 767, 25, doi: [10.1088/0004-637X/767/1/25](https://doi.org/10.1088/0004-637X/767/1/25)
- Guo, F., Li, X., Li, H., et al. 2016, *ApJL*, 818, L9, doi: [10.3847/2041-8205/818/1/L9](https://doi.org/10.3847/2041-8205/818/1/L9)

- Guo, H., Sun, J., Li, S.-L., et al. 2023a, arXiv e-prints, arXiv:2312.06771, doi: [10.48550/arXiv.2312.06771](https://doi.org/10.48550/arXiv.2312.06771)
- Guo, W.-J., Li, Y.-R., Zhang, Z.-X., Ho, L. C., & Wang, J.-M. 2022, *ApJ*, 929, 19, doi: [10.3847/1538-4357/ac4e84](https://doi.org/10.3847/1538-4357/ac4e84)
- Guo, W.-J., Zou, H., Fawcett, V. A., et al. 2023b, arXiv e-prints, arXiv:2307.08289, doi: [10.48550/arXiv.2307.08289](https://doi.org/10.48550/arXiv.2307.08289)
- Guo, W.-J., Zou, H., Greenwell, C. L., et al. 2024, arXiv e-prints, arXiv:2408.00402, doi: [10.48550/arXiv.2408.00402](https://doi.org/10.48550/arXiv.2408.00402)
- Hammerstein, E., van Velzen, S., Gezari, S., et al. 2023, *ApJ*, 942, 9, doi: [10.3847/1538-4357/aca283](https://doi.org/10.3847/1538-4357/aca283)
- Hinkle, J. T., Shappee, B. J., Auchettl, K., et al. 2024, arXiv e-prints, arXiv:2405.08855, doi: [10.48550/arXiv.2405.08855](https://doi.org/10.48550/arXiv.2405.08855)
- Holoien, T. W. S., Neustadt, J. M. M., Vallely, P. J., et al. 2022, *ApJ*, 933, 196, doi: [10.3847/1538-4357/ac74b9](https://doi.org/10.3847/1538-4357/ac74b9)
- Hopkins, P. F., Hernquist, L., Cox, T. J., et al. 2006, *ApJS*, 163, 1, doi: [10.1086/499298](https://doi.org/10.1086/499298)
- Hosseinzadeh, G., Berger, E., Metzger, B. D., et al. 2022, *ApJ*, 933, 14, doi: [10.3847/1538-4357/ac67dd](https://doi.org/10.3847/1538-4357/ac67dd)
- Hovatta, T., & Lindfors, E. 2019, *NewAR*, 87, 101541, doi: [10.1016/j.newar.2020.101541](https://doi.org/10.1016/j.newar.2020.101541)
- Huang, Y.-K., Hu, C., Zhao, Y.-L., et al. 2019, *ApJ*, 876, 102, doi: [10.3847/1538-4357/ab16ef](https://doi.org/10.3847/1538-4357/ab16ef)
- Hughes, P. A., Aller, H. D., & Aller, M. F. 1985, *ApJ*, 298, 301, doi: [10.1086/163611](https://doi.org/10.1086/163611)
- Inserra, C., Smartt, S. J., Gall, E. E. E., et al. 2018, *MNRAS*, 475, 1046, doi: [10.1093/mnras/stx3179](https://doi.org/10.1093/mnras/stx3179)
- Jiang, L., Fan, X., & Vestergaard, M. 2008, *ApJ*, 679, 962, doi: [10.1086/587868](https://doi.org/10.1086/587868)
- Jiang, N., Wang, T., Mou, G., et al. 2019, *ApJ*, 871, 15, doi: [10.3847/1538-4357/aaf6b2](https://doi.org/10.3847/1538-4357/aaf6b2)
- Jiang, N., Wang, T., Yan, L., et al. 2017, *ApJ*, 850, 63, doi: [10.3847/1538-4357/aa93f5](https://doi.org/10.3847/1538-4357/aa93f5)
- Kagan, D., Sironi, L., Cerutti, B., & Giannios, D. 2015, *SSRv*, 191, 545, doi: [10.1007/s11214-014-0132-9](https://doi.org/10.1007/s11214-014-0132-9)
- Kankare, E., Kotak, R., Mattila, S., et al. 2017, *Nature Astronomy*, 1, 865, doi: [10.1038/s41550-017-0290-2](https://doi.org/10.1038/s41550-017-0290-2)
- Kara, E., Mehdipour, M., Kriss, G. A., et al. 2021, arXiv e-prints, arXiv:2105.05840. <https://arxiv.org/abs/2105.05840>
- Karas, V., & Šubr, L. 2007, *A&A*, 470, 11, doi: [10.1051/0004-6361/20066068](https://doi.org/10.1051/0004-6361/20066068)
- Kaur, K., & Stone, N. C. 2024, arXiv e-prints, arXiv:2405.18500, doi: [10.48550/arXiv.2405.18500](https://doi.org/10.48550/arXiv.2405.18500)
- Kelly, B. C., Bechtold, J., & Siemiginowska, A. 2009, *ApJ*, 698, 895, doi: [10.1088/0004-637X/698/1/895](https://doi.org/10.1088/0004-637X/698/1/895)
- Kochanek, C. S. 2016, *MNRAS*, 458, 127, doi: [10.1093/mnras/stw267](https://doi.org/10.1093/mnras/stw267)
- Kochanek, C. S., Shappee, B. J., Stanek, K. Z., et al. 2017, *PASP*, 129, 104502, doi: [10.1088/1538-3873/aa80d9](https://doi.org/10.1088/1538-3873/aa80d9)
- Komossa, S., Voges, W., Xu, D., et al. 2006, *AJ*, 132, 531, doi: [10.1086/505043](https://doi.org/10.1086/505043)
- Konigl, A. 1981, *ApJ*, 243, 700, doi: [10.1086/158638](https://doi.org/10.1086/158638)
- Kool, E. C., Reynolds, T. M., Mattila, S., et al. 2020, *MNRAS*, 498, 2167, doi: [10.1093/mnras/staa2351](https://doi.org/10.1093/mnras/staa2351)
- Koshida, S., Minezaki, T., Yoshii, Y., et al. 2014, *ApJ*, 788, 159, doi: [10.1088/0004-637X/788/2/159](https://doi.org/10.1088/0004-637X/788/2/159)
- Kozłowski, S., Kochanek, C. S., Udalski, A., et al. 2010, *ApJ*, 708, 927, doi: [10.1088/0004-637X/708/2/927](https://doi.org/10.1088/0004-637X/708/2/927)
- Krolik, J. H., Horne, K., Kallman, T. R., et al. 1991, *ApJ*, 371, 541, doi: [10.1086/169918](https://doi.org/10.1086/169918)
- Larionov, V. M., Jorstad, S. G., Marscher, A. P., et al. 2013, *ApJ*, 768, 40, doi: [10.1088/0004-637X/768/1/40](https://doi.org/10.1088/0004-637X/768/1/40)
- Leloudas, G., Dai, L., Arcavi, I., et al. 2019, *ApJ*, 887, 218, doi: [10.3847/1538-4357/ab5792](https://doi.org/10.3847/1538-4357/ab5792)
- Li, Y.-R., Wang, J.-M., Hu, C., Du, P., & Bai, J.-M. 2014, *ApJL*, 786, L6, doi: [10.1088/2041-8205/786/1/L6](https://doi.org/10.1088/2041-8205/786/1/L6)
- Liao, N.-H., Dou, L.-M., Jiang, N., et al. 2019, *ApJL*, 879, L9, doi: [10.3847/2041-8213/ab2893](https://doi.org/10.3847/2041-8213/ab2893)
- Lin, D. N. C., & Shields, G. A. 1986, *ApJ*, 305, 28, doi: [10.1086/164225](https://doi.org/10.1086/164225)
- Lioudakis, I., Romani, R. W., Filippenko, A. V., Kocevski, D., & Zheng, W. 2019, *ApJ*, 880, 32, doi: [10.3847/1538-4357/ab26b7](https://doi.org/10.3847/1538-4357/ab26b7)
- Liu, X., Dittmann, A., Shen, Y., & Jiang, L. 2018, *ApJ*, 859, 8, doi: [10.3847/1538-4357/aabb04](https://doi.org/10.3847/1538-4357/aabb04)
- Liu, Z., Malyali, A., Krumpe, M., et al. 2023, *A&A*, 669, A75, doi: [10.1051/0004-6361/202244805](https://doi.org/10.1051/0004-6361/202244805)
- Loeb, A., & Ulmer, A. 1997, *ApJ*, 489, 573, doi: [10.1086/304814](https://doi.org/10.1086/304814)
- Lu, W., Kumar, P., & Evans, N. J. 2016, *MNRAS*, 458, 575, doi: [10.1093/mnras/stw307](https://doi.org/10.1093/mnras/stw307)
- Lyu, J., Rieke, G. H., & Smith, P. S. 2019, *ApJ*, 886, 33, doi: [10.3847/1538-4357/ab481d](https://doi.org/10.3847/1538-4357/ab481d)
- MacLeod, C. L., Ivezić, Ž., Kochanek, C. S., et al. 2010, *ApJ*, 721, 1014, doi: [10.1088/0004-637X/721/2/1014](https://doi.org/10.1088/0004-637X/721/2/1014)
- MacLeod, C. L., Green, P. J., Anderson, S. F., et al. 2019, *ApJ*, 874, 8, doi: [10.3847/1538-4357/ab05e2](https://doi.org/10.3847/1538-4357/ab05e2)
- MacLeod, M., Ramirez-Ruiz, E., Grady, S., & Guillochon, J. 2013, *ApJ*, 777, 133, doi: [10.1088/0004-637X/777/2/133](https://doi.org/10.1088/0004-637X/777/2/133)
- Mainetti, D., Lupi, A., Campana, S., et al. 2017, *A&A*, 600, A124, doi: [10.1051/0004-6361/201630092](https://doi.org/10.1051/0004-6361/201630092)
- Makrygianni, L., Trakhtenbrot, B., Arcavi, I., et al. 2023, *ApJ*, 953, 32, doi: [10.3847/1538-4357/ace1ee](https://doi.org/10.3847/1538-4357/ace1ee)
- Malyali, A., Rau, A., Merloni, A., et al. 2021, *A&A*, 647, A9, doi: [10.1051/0004-6361/202039681](https://doi.org/10.1051/0004-6361/202039681)
- Malyali, A., Liu, Z., Rau, A., et al. 2023, *MNRAS*, 520, 3549, doi: [10.1093/mnras/stad022](https://doi.org/10.1093/mnras/stad022)
- Marscher, A. P., & Gear, W. K. 1985, *ApJ*, 298, 114, doi: [10.1086/163592](https://doi.org/10.1086/163592)
- Masci, F. J., Laher, R. R., Rusholme, B., et al. 2019, *PASP*, 131, 018003, doi: [10.1088/1538-3873/aae8ac](https://doi.org/10.1088/1538-3873/aae8ac)
- Mattila, S., Pérez-Torres, M., Efstathiou, A., et al. 2018, *Science*, 361, 482, doi: [10.1126/science.aao4669](https://doi.org/10.1126/science.aao4669)

- McKernan, B., Ford, K. E. S., Cantiello, M., et al. 2022, *MNRAS*, 514, 4102, doi: [10.1093/mnras/stac1310](https://doi.org/10.1093/mnras/stac1310)
- Merloni, A., Dwelly, T., Salvato, M., et al. 2015, *MNRAS*, 452, 69, doi: [10.1093/mnras/stv1095](https://doi.org/10.1093/mnras/stv1095)
- Metzger, B. D. 2022, *ApJL*, 937, L12, doi: [10.3847/2041-8213/ac90ba](https://doi.org/10.3847/2041-8213/ac90ba)
- Metzger, B. D., & Stone, N. C. 2016, *MNRAS*, 461, 948, doi: [10.1093/mnras/stw1394](https://doi.org/10.1093/mnras/stw1394)
- Miles, P. R., Coughlin, E. R., & Nixon, C. J. 2020, *ApJ*, 899, 36, doi: [10.3847/1538-4357/ab9c9f](https://doi.org/10.3847/1538-4357/ab9c9f)
- Miller, A. A., Chornock, R., Perley, D. A., et al. 2009, *ApJ*, 690, 1303, doi: [10.1088/0004-637X/690/2/1303](https://doi.org/10.1088/0004-637X/690/2/1303)
- Miller, M. C. 2015, *ApJ*, 805, 83, doi: [10.1088/0004-637X/805/1/83](https://doi.org/10.1088/0004-637X/805/1/83)
- Minezaki, T., Yoshii, Y., Kobayashi, Y., et al. 2019, *ApJ*, 886, 150, doi: [10.3847/1538-4357/ab4f7b](https://doi.org/10.3847/1538-4357/ab4f7b)
- Mockler, B., Gallegos-Garcia, M., Götberg, Y., Miller, J., & Ramirez-Ruiz, E. 2024, arXiv e-prints, arXiv:2406.04455, doi: [10.48550/arXiv.2406.04455](https://doi.org/10.48550/arXiv.2406.04455)
- Netzer, H. 2013, *The Physics and Evolution of Active Galactic Nuclei*
- Netzer, H., Elitzur, M., & Ferland, G. J. 1985, *ApJ*, 299, 752, doi: [10.1086/163741](https://doi.org/10.1086/163741)
- Neugebauer, G., & Matthews, K. 1999, *AJ*, 118, 35, doi: [10.1086/300945](https://doi.org/10.1086/300945)
- Neustadt, J. M. M., Holoiën, T. W. S., Kochanek, C. S., et al. 2020, *MNRAS*, 494, 2538, doi: [10.1093/mnras/staa859](https://doi.org/10.1093/mnras/staa859)
- Nicholl, M., Short, P., Lawrence, A., Ross, N., & Smartt, S. 2019, *Transient Name Server Classification Report, 2019-1586*, 1
- Osmer, P. S. 1980, *ApJ*, 237, 666, doi: [10.1086/157913](https://doi.org/10.1086/157913)
- Osterbrock, D. E. 1974, *Astrophysics of gaseous nebulae*
- Paltani, S., Courvoisier, T. J. L., Blecha, A., & Bratschi, P. 1997, *A&A*, 327, 539, doi: [10.48550/arXiv.astro-ph/9706203](https://doi.org/10.48550/arXiv.astro-ph/9706203)
- Payne, A. V., Shappee, B. J., Hinkle, J. T., et al. 2021, *ApJ*, 910, 125, doi: [10.3847/1538-4357/abe38d](https://doi.org/10.3847/1538-4357/abe38d)
- Perger, K., Frey, S., & Gabányi, K. É. 2023, *Ap&SS*, 368, 18, doi: [10.1007/s10509-023-04176-4](https://doi.org/10.1007/s10509-023-04176-4)
- Peterson, B. M. 1993, *PASP*, 105, 247, doi: [10.1086/133140](https://doi.org/10.1086/133140)
- Peterson, B. M., Wanders, I., Horne, K., et al. 1998, *PASP*, 110, 660, doi: [10.1086/316177](https://doi.org/10.1086/316177)
- Petrushevska, T., Leloudas, G., Ilić, D., et al. 2023, *A&A*, 669, A140, doi: [10.1051/0004-6361/202244623](https://doi.org/10.1051/0004-6361/202244623)
- Phinney, E. S. 1989, in *The Center of the Galaxy*, ed. M. Morris, Vol. 136, 543
- Piran, T., Svirski, G., Krolik, J., Cheng, R. M., & Shiokawa, H. 2015, *ApJ*, 806, 164, doi: [10.1088/0004-637X/806/2/164](https://doi.org/10.1088/0004-637X/806/2/164)
- Planck Collaboration, Aghanim, N., Akrami, Y., et al. 2020, *A&A*, 641, A6, doi: [10.1051/0004-6361/201833910](https://doi.org/10.1051/0004-6361/201833910)
- Prasad, C., Wang, Y., Perna, R., Ford, K. E. S., & McKernan, B. 2024, *MNRAS*, 531, 1409, doi: [10.1093/mnras/stae1263](https://doi.org/10.1093/mnras/stae1263)
- Raiteri, C. M., Villata, M., Tosti, G., et al. 2003, *A&A*, 402, 151, doi: [10.1051/0004-6361:20030256](https://doi.org/10.1051/0004-6361:20030256)
- Raiteri, C. M., Villata, M., Kadler, M., et al. 2006, *A&A*, 459, 731, doi: [10.1051/0004-6361:20065744](https://doi.org/10.1051/0004-6361:20065744)
- Rakshit, S., Stalin, C. S., Chand, H., & Zhang, X.-G. 2017, *ApJS*, 229, 39, doi: [10.3847/1538-4365/aa6971](https://doi.org/10.3847/1538-4365/aa6971)
- Rani, B., Gupta, A. C., Joshi, U. C., Ganesh, S., & Wiita, P. J. 2010, *ApJL*, 719, L153, doi: [10.1088/2041-8205/719/2/L153](https://doi.org/10.1088/2041-8205/719/2/L153)
- Rani, B., Krichbaum, T. P., Fuhrmann, L., et al. 2013, *A&A*, 552, A11, doi: [10.1051/0004-6361/201321058](https://doi.org/10.1051/0004-6361/201321058)
- Rees, M. J. 1988, *Nature*, 333, 523, doi: [10.1038/333523a0](https://doi.org/10.1038/333523a0)
- Reynolds, T. M., Mattila, S., Efstathiou, A., et al. 2022, *A&A*, 664, A158, doi: [10.1051/0004-6361/202243289](https://doi.org/10.1051/0004-6361/202243289)
- Ricci, C., & Trakhtenbrot, B. 2023, *Nature Astronomy*, 7, 1282, doi: [10.1038/s41550-023-02108-4](https://doi.org/10.1038/s41550-023-02108-4)
- Roth, N., & Kasen, D. 2018, *ApJ*, 855, 54, doi: [10.3847/1538-4357/aaac6c](https://doi.org/10.3847/1538-4357/aaac6c)
- Roth, N., Kasen, D., Guillochon, J., & Ramirez-Ruiz, E. 2016, *ApJ*, 827, 3, doi: [10.3847/0004-637X/827/1/3](https://doi.org/10.3847/0004-637X/827/1/3)
- Sanders, D. B., Soifer, B. T., Elias, J. H., Neugebauer, G., & Matthews, K. 1988, *ApJL*, 328, L35, doi: [10.1086/185155](https://doi.org/10.1086/185155)
- Shiokawa, H., Krolik, J. H., Cheng, R. M., Piran, T., & Noble, S. C. 2015, *ApJ*, 804, 85, doi: [10.1088/0004-637X/804/2/85](https://doi.org/10.1088/0004-637X/804/2/85)
- Singh, V., & Chand, H. 2018, *MNRAS*, 480, 1796, doi: [10.1093/mnras/sty1818](https://doi.org/10.1093/mnras/sty1818)
- Somalwar, J. J., Ravi, V., Yao, Y., et al. 2023, arXiv e-prints, arXiv:2310.03782, doi: [10.48550/arXiv.2310.03782](https://doi.org/10.48550/arXiv.2310.03782)
- Soraisam, M., Matheson, T., Lee, C.-H., et al. 2022, *ApJL*, 926, L11, doi: [10.3847/2041-8213/ac4e99](https://doi.org/10.3847/2041-8213/ac4e99)
- Stern, D., Eisenhardt, P., Gorjian, V., et al. 2005, *ApJ*, 631, 163, doi: [10.1086/432523](https://doi.org/10.1086/432523)
- Stern, D., Assef, R. J., Benford, D. J., et al. 2012, *ApJ*, 753, 30, doi: [10.1088/0004-637X/753/1/30](https://doi.org/10.1088/0004-637X/753/1/30)
- Stone, N., Sari, R., & Loeb, A. 2013, *MNRAS*, 435, 1809, doi: [10.1093/mnras/stt1270](https://doi.org/10.1093/mnras/stt1270)
- Stone, N. C., & van Velzen, S. 2016, *ApJL*, 825, L14, doi: [10.3847/2041-8205/825/1/L14](https://doi.org/10.3847/2041-8205/825/1/L14)
- Sun, L., Jiang, N., Dou, L., et al. 2024, arXiv e-prints, arXiv:2410.09720, doi: [10.48550/arXiv.2410.09720](https://doi.org/10.48550/arXiv.2410.09720)
- Tadhunter, C., Spence, R., Rose, M., Mullaney, J., & Crowther, P. 2017, *Nature Astronomy*, 1, 0061, doi: [10.1038/s41550-017-0061](https://doi.org/10.1038/s41550-017-0061)
- Terreran, G., Berton, M., Benetti, S., et al. 2016, *The Astronomer's Telegram*, 9417, 1
- Tonry, J. L., Denneau, L., Heinze, A. N., et al. 2018, *PASP*, 130, 064505, doi: [10.1088/1538-3873/aabadf](https://doi.org/10.1088/1538-3873/aabadf)
- Trakhtenbrot, B., Arcavi, I., Ricci, C., et al. 2019, *Nature Astronomy*, 3, 242, doi: [10.1038/s41550-018-0661-3](https://doi.org/10.1038/s41550-018-0661-3)
- Urry, C. M., & Mushotzky, R. F. 1982, *ApJ*, 253, 38, doi: [10.1086/159607](https://doi.org/10.1086/159607)

- van Velzen, S., Holoiën, T. W. S., Onori, F., Hung, T., & Arcavi, I. 2020, *SSRv*, 216, 124, doi: [10.1007/s11214-020-00753-z](https://doi.org/10.1007/s11214-020-00753-z)
- van Velzen, S., Farrar, G. R., Gezari, S., et al. 2011, *ApJ*, 741, 73, doi: [10.1088/0004-637X/741/2/73](https://doi.org/10.1088/0004-637X/741/2/73)
- van Velzen, S., Gezari, S., Cenko, S. B., et al. 2019, *ApJ*, 872, 198, doi: [10.3847/1538-4357/aafe0c](https://doi.org/10.3847/1538-4357/aafe0c)
- van Velzen, S., Gezari, S., Hammerstein, E., et al. 2021, *ApJ*, 908, 4, doi: [10.3847/1538-4357/abc258](https://doi.org/10.3847/1538-4357/abc258)
- Vanden Berk, D. E., Richards, G. T., Bauer, A., et al. 2001, *AJ*, 122, 549, doi: [10.1086/321167](https://doi.org/10.1086/321167)
- Vaona, L., Ciroi, S., Di Mille, F., et al. 2012, *MNRAS*, 427, 1266, doi: [10.1111/j.1365-2966.2012.22060.x](https://doi.org/10.1111/j.1365-2966.2012.22060.x)
- Veilleux, S., & Osterbrock, D. E. 1987, *ApJS*, 63, 295, doi: [10.1086/191166](https://doi.org/10.1086/191166)
- Veres, P. M., Franckowiak, A., van Velzen, S., et al. 2024, Back from the dead: AT2019aal as a candidate repeating TDE in an AGN. <https://arxiv.org/abs/2408.17419>
- Wang, J.-M., Ge, J.-Q., Hu, C., et al. 2011, *ApJ*, 739, 3, doi: [10.1088/0004-637X/739/1/3](https://doi.org/10.1088/0004-637X/739/1/3)
- Wang, J.-M., Du, P., Hu, C., et al. 2014, *ApJ*, 793, 108, doi: [10.1088/0004-637X/793/2/108](https://doi.org/10.1088/0004-637X/793/2/108)
- Wang, Y., Lin, D. N. C., Zhang, B., & Zhu, Z. 2024, *ApJL*, 962, L7, doi: [10.3847/2041-8213/ad20e5](https://doi.org/10.3847/2041-8213/ad20e5)
- Wevers, T., Coughlin, E. R., Pasham, D. R., et al. 2023, *ApJL*, 942, L33, doi: [10.3847/2041-8213/ac9f36](https://doi.org/10.3847/2041-8213/ac9f36)
- Whalen, D. J., Laurent-Muehleisen, S. A., Moran, E. C., & Becker, R. H. 2006, *AJ*, 131, 1948, doi: [10.1086/500825](https://doi.org/10.1086/500825)
- White, R. L., Becker, R. H., Gregg, M. D., et al. 2000, *ApJS*, 126, 133, doi: [10.1086/313300](https://doi.org/10.1086/313300)
- Wiseman, P., Williams, R. D., Arcavi, I., et al. 2024, arXiv e-prints, arXiv:2406.11552, doi: [10.48550/arXiv.2406.11552](https://doi.org/10.48550/arXiv.2406.11552)
- Wolfe, A. M. 1978, Pittsburgh Conference on BL LAC Objects, Held at the University of Pittsburgh, April 24-26, 1978: [Papers] No. xiii, 428 p. (Pittsburgh: University of Pittsburgh, Dept. of Physics and Astronomy)
- Woo, J.-H., Treu, T., Barth, A. J., et al. 2010, *ApJ*, 716, 269, doi: [10.1088/0004-637X/716/1/269](https://doi.org/10.1088/0004-637X/716/1/269)
- Wu, X.-J., & Yuan, Y.-F. 2018, *MNRAS*, 479, 1569, doi: [10.1093/mnras/sty1423](https://doi.org/10.1093/mnras/sty1423)
- Yang, Q., Shen, Y., Liu, X., et al. 2019, *ApJ*, 885, 110, doi: [10.3847/1538-4357/ab481a](https://doi.org/10.3847/1538-4357/ab481a)
- Yao, Y., Ravi, V., Gezari, S., et al. 2023, *ApJL*, 955, L6, doi: [10.3847/2041-8213/acf216](https://doi.org/10.3847/2041-8213/acf216)
- Zacharias, M., Böttcher, M., Jankowsky, F., et al. 2017, *ApJ*, 851, 72, doi: [10.3847/1538-4357/aa9bee](https://doi.org/10.3847/1538-4357/aa9bee)
- Zhong, S., Li, S., Berczik, P., & Spurzem, R. 2022, *ApJ*, 933, 96, doi: [10.3847/1538-4357/ac71ad](https://doi.org/10.3847/1538-4357/ac71ad)
- Zhou, H., Wang, T., Yuan, W., et al. 2006, *ApJS*, 166, 128, doi: [10.1086/504869](https://doi.org/10.1086/504869)
- Zhuang, M.-Y., & Ho, L. C. 2020, *ApJ*, 896, 108, doi: [10.3847/1538-4357/ab8f2e](https://doi.org/10.3847/1538-4357/ab8f2e)
- Zu, Y., Kochanek, C. S., Kozłowski, S., & Udalski, A. 2013, *ApJ*, 765, 106, doi: [10.1088/0004-637X/765/2/106](https://doi.org/10.1088/0004-637X/765/2/106)